Technical Report Documentation Page

1. Report No. FHWA/TX-0-1814-1	2. Government Accession No.	3. Recipient's Catalog No.
4. Title and Subtitle REPORT ON A COMPARISON OF THE EFFECTIVENESS OF TWO PAVEMENT REHABILITATION STRATEGIES ON US 281 NEAR JACKSBORO		5. Report Date December 1999 Revised: May 2001
7. Author(s) Fred Hugo, Dar-Hao Chen, André de Fortier Smit, and John Bilyeu		6. Performing Organization Code 8. Performing Organization Report No. 0-1814-1
9. Performing Organization Name and Address Center for Transportation Research The University of Texas at Austin 3208 Red River, Suite 200 Austin, TX 78705-2650		10. Work Unit No. (TRAIS) 11. Contract or Grant No. 0-1814
12. Sponsoring Agency Name and Address Texas Department of Transportation Research and Technology Implementation Office P.O. Box 5080 Austin, TX 78763-5080		13. Type of Report and Period Covered Research Report (9/1/98 to 8/31/99) 14. Sponsoring Agency Code

15. Supplementary Notes

Project conducted in cooperation with the Texas Department of Transportation, U.S. Department of Transportation, and the Federal Highway Administration.

16. Abstract

The main objective of the most recent MLS test program was to conduct a comparative study of two rehabilitation processes, Remixer and Dustrol, constructed on the southbound and northbound lanes of US 281 near Jacksboro, Texas, in the Fort Worth District, in 1995 and 1996, respectively. The underlying pavements are composite asphalt layers, with the first construction undertaken in 1957.

Since no temperature control was provided during trafficking, the tests were conducted in consecutive, similar seasons to reduce variability induced by temperature changes. Performance was evaluated in terms of surface rutting, loss of stiffness in pavement layers, and permanent deformation in the layers. Tools used during the study included an on-site weather station, nondestructive testing equipment (GPR, FWD, SPA, PSPA, SASW, DCP), in-situ instrumentation (MDD), and the Hamburg wheel-tracking device. The findings provided conclusive results on the relative performance of the two rehab strategies. The results indicated that the Remixer process performs better than the Dustrol process on resisting rutting, although both mixes are stable, with no sign of premature failure. Based on the good performance of the Remixer rehab on its sound underlying structure, it was used on a section of US 175 in the Dallas District. However it was found later that the Remixer could not stop reflected cracking on the US 175 project.

17. Key Words: Texas Mobile Load Simulator, accelerated pavement testing	18. Distribution Statement No restrictions. This document is available to the public through the National Technical Information Service, Springfield, Virginia 22161.		
19. Security Classif. (of report) Unclassified	20. Security Classif. (of this page) Unclassified	21. No. of pages 62	22. Price

Form DOT F 1700.7 (8-72) Reproduction of completed page authorized

REPORT ON A COMPARISON OF THE EFFECTIVENESS OF TWO PAVEMENT REHABILITATION STRATEGIES ON US 281 NEAR JACKSBORO

by

Fred Hugo, Dar-Hao Chen, André de Fortier Smit, and John Bilyeu

Research Report Number 0-1814-1

Research Project 0-1814
MLS Research Management System – Phase II

Conducted for the

TEXAS DEPARTMENT OF TRANSPORTATION

in cooperation with the

U.S. DEPARTMENT OF TRANSPORTATION
FEDERAL HIGHWAY ADMINISTRATION

by the

CENTER FOR TRANSPORTATION RESEARCH
Bureau of Engineering Research
THE UNIVERSITY OF TEXAS AT AUSTIN

and the

TEXAS TRANSPORTATION INSTITUTE
TEXAS A&M UNIVERSITY SYSTEM
and
THE UNIVERSITY OF TEXAS AT EL PASO

December 1999
Revised: May 2001

DISCLAIMERS

The contents of this report reflect the views of the authors, who are responsible for the facts and the accuracy of the data presented herein. The contents do not necessarily reflect the official views or policies of either the Federal Highway Administration (FHWA) or the Texas Department of Transportation (TxDOT). This report does not constitute a standard, specification, or regulation.

There was no invention or discovery conceived or first actually reduced to practice in the course of or under this contract, including any art, method, process, machine, manufacture, design or composition of matter, or any new and useful improvement thereof, or any variety of plant, which is or may be patentable under the patent laws of the United States of America or any foreign country.

NOT INTENDED FOR CONSTRUCTION, BIDDING, OR PERMIT PURPOSES

Frederick Hugo, P.E. (Texas No. 67246)
Research Supervisor

ACKNOWLEDGMENTS

The researchers appreciate the assistance provided by Mr. Ken Fults, P.E. (DES), who served as the project director for this study until he was succeeded by Dr. Mike Murphy, P.E. (DES). Research was performed in cooperation with TxDOT.

The authors would also like to express their sincere appreciation to Mr. Ken Fults, Dr. Mike Murphy, and Dr. Andrew Wimsatt for their input and suggestions, and to Mr. Tom Scullion, Mr. John Ragsdale, Dr. Soheil Nazarian, and Dr. Deren Yuan for their assistance with MDD and PSPA analyses.

Research performed in cooperation with the Texas Department of Transportation and the U.S. Department of Transportation, Federal Highway Administration

ABSTRACT

The main objective of the most recent MLS test program was to conduct a comparative study of two rehabilitation processes — Remixer and Dustrol — constructed on the southbound and northbound lanes of US 281 near Jacksboro, Texas, in the Fort Worth District, in 1995 and 1996, respectively. The underlying pavements are composite asphalt layers, with the first construction done in 1957.

Because no temperature control was provided during trafficking, the tests were conducted in consecutive, similar seasons to reduce variability induced by temperature changes. Performance was evaluated in terms of surface rutting, loss of stiffness in pavement layers, and permanent deformation in the layers. Tools used during the study included an on-site weather station, nondestructive testing equipment (GPR, FWD, SPA, PSPA, SASW, and DCP), in-situ instrumentation (MDD), and the Hamburg wheel-tracking device.

The findings provided conclusive results on the relative performance of the two rehab strategies. The results indicated that the Remixer process performs better than the Dustrol process, although both mixes are stable, with no sign of premature failure. Despite the satisfactory performance of the Remixer overlay, severe distress in the form of longitudinal and alligator cracking manifested itself in the outside lane adjacent to the test section during the execution of the S1 test. This distress was ascribed to stripping in the underlying lightweight asphalt concrete (LWAC) and possible weakness of the underlying structure. Water susceptibility and the effects of high temperature trafficking were subsequently investigated using the one-third-scale Model Mobile Load Simulator (MMLS3). Based on the satisfactory performance of the Remixer rehab on its sound underlying structure, it was used on a section of US 175 in the Dallas District. However it was found later that the Remixer could not stop reflected cracking on the US 175 project.

TABLE OF CONTENTS

INTRODUCTION

This report presents the field and analytical results of the most recent comparative study of an in-service pavement section on US 281 in Jacksboro, Texas.

THE TEXAS MOBILE LOAD SIMULATOR (MLS)

Accelerated pavement testing (APT) with the Texas Mobile Load Simulator (MLS) enables pavement engineers to gain insight into pavement-related distress over a relatively short period. To accelerate pavement wear, the MLS, shown in Figure 1, is operated nominally at 11 mph and achieves an average 6,000 axle repetitions per hour.

The MLS is equipped with six full, standard tandem axles that travel in one direction. The standard test procedure uses legal tandem axle loads of 34,000 lb. The axle repetitions mentioned in this report represent half of a tandem axle, or one 17,000-lb axle. There is a total of forty-eight tires; each is inflated to approximately 100 psi. The dimensions of the MLS are nominally 100 ft long by 20 ft tall by 15 ft wide.* A more detailed discussion of the TxMLS can be found elsewhere (Metcalf, 1996; Chen et al., 1997; Chen and Hugo, 1998). A summary of TxMLS features is contained in Table 1.

TEST SECTION

The test sections are in-service pavements located on US 281 near Jacksboro, Texas, in the Fort Worth District. The lengths of both rehabilitated pavements are approximately 5 miles. US 281 is a divided, four-lane highway with a 10 ft shoulder on the outside and a 4 ft shoulder on the inside lane in each direction. The Fort Worth District Pavement Engineer indicated that an average of 3,100 vehicles per day (1,550 per direction) traveled the highway in 1994. Approximately 17.4 percent of these vehicles were trucks. Approximately 10 percent of all traffic travels on the inside lane.

Site Selection

It was important to select test sites with similar characteristics. Nondestructive testing was conducted to assist in site selection. Data collected during site selection included the following:

(1) visual surface distress (rutting and cracking);

(2) structural conditions measured by Falling Weight Deflectometer (FWD), Portable Seismic Pavement Analyzer (PSPA), Seismic Pavement Analyzer (SPA), Spectral Analysis of Surface Waves (SASW), and Ground Penetrating Radar (GPR);

(3) topography (the MLS requires a nearly flat surface to maintain uniform loads); and

(4) subsurface condition (underlying cracks, layer thickness) based on GPR results, Dynamic Cone Penetrometer (DCP) and use of seismic refraction techniques.

---

* Research data and findings in the field of accelerated pavement testing (APT) are normally reported in metric units in accordance with a decision by the TRB committee A2B09 on Full-Scale Accelerated Pavement Testing.

Because of the nature of the study, this report has conventional English units. In cases where metric units are more appropriate, they have been added as the primary units.

(a) Overview of the MLS Site

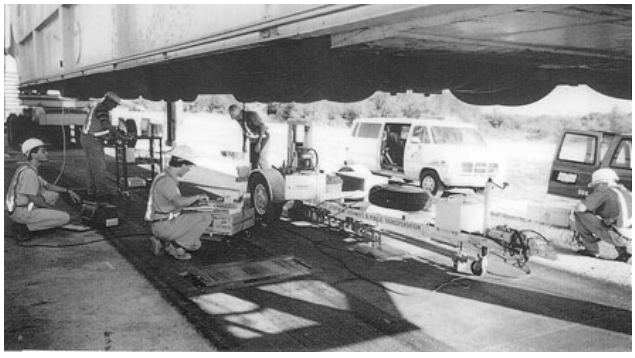

(b) Surveillance under the MLS

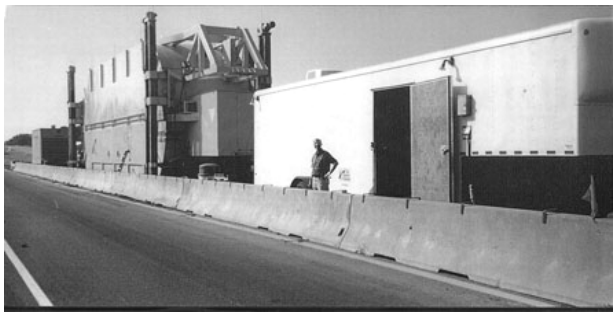

(c) Traffic Lane alongside the MLS

Figure 1 The MLS Testing on US 281, Jacksboro

The nondestructive testing (FWD, SPA, SASW, and GPR) data served as diagnostic tools for determining the present structural condition. GPR results are presented by Wimsatt et al. (1998). Aspects of the study are also presented by Hugo et al. (1997).

After evaluation of the data, four 40-ft sections with similar material characteristics were selected. Although four sections were tested, only the tests related to the comparative study are presented here. The rehab processes discussed in this paper, Remixer and Dustrol, refer to the strategies employed in the southbound (281 S1) and northbound (281 N1) lanes, respectively.

Table 1 TxMLS Configuration and Other Characteristics

FEATURE	TECHNICAL DATA
No. of bogies	6
No. of axles/bogie	2 (dual tandems)
Total no. of full axles	12
• Drive axles	2
• Towed axles	10
No. of wheels	24 duals
Tires/axle	4
Tire type	295 x 75R22.5 Low profile radial
Tire pressure (psi)	100
Nominal tire tread width (in.)	9
Nominal distance between tire centerlines (in.)	13
Nominal wheel diameter (in.)	39.4
Nominal load per axle (kip)	17
Nominal load per wheel (lb)	4250
Load mechanism	Conventional highway truck springs
Load setting	Electro-mechanical (+/- 100 lbs)
Suspension	Steel springs
Nominal speed (uni-directional travel of axles) mph	11
Duration of load pulse at operational speed (sec)	0.05s
Nominal rest periods between load applications (sec)	Rest periods vary among 0.2s, 0.74s, and 1.74s
Nominal time per cycle (sec)	8
Power	2 x 160 hp DC motors
Maximum production rate/12 h shift (No. of axles)	>50,000
Lateral wander (overall left to right) (in.)	17
Mobility	Tractor towed supported on special bogies
Length (ft)	100
Width (ft)	15
Height (ft)	20
Total nominal mass (ton)	134
Test section size [width x length] (ft)	~10 x ~40 (3 m x 12 m)
Temp control during tests	None, except for cover by structural shell

Pavement Condition and History

The first asphalt layer of the test section was constructed in 1957. Four major overlays/rehabilitations were completed in 1971, 1976, 1986, and 1995. Figure 2 shows the complete pavement history. In 1986, there was a major rehabilitation using 3 in. of lightweight-aggregate asphalt concrete (LWAC) on the southbound lane, and 2 to 2.4 in. on the northbound lane. The pavement structure comprises 6.9 to 8 in. total asphaltic concrete (AC) and a crushed aggregate base of 15 in.

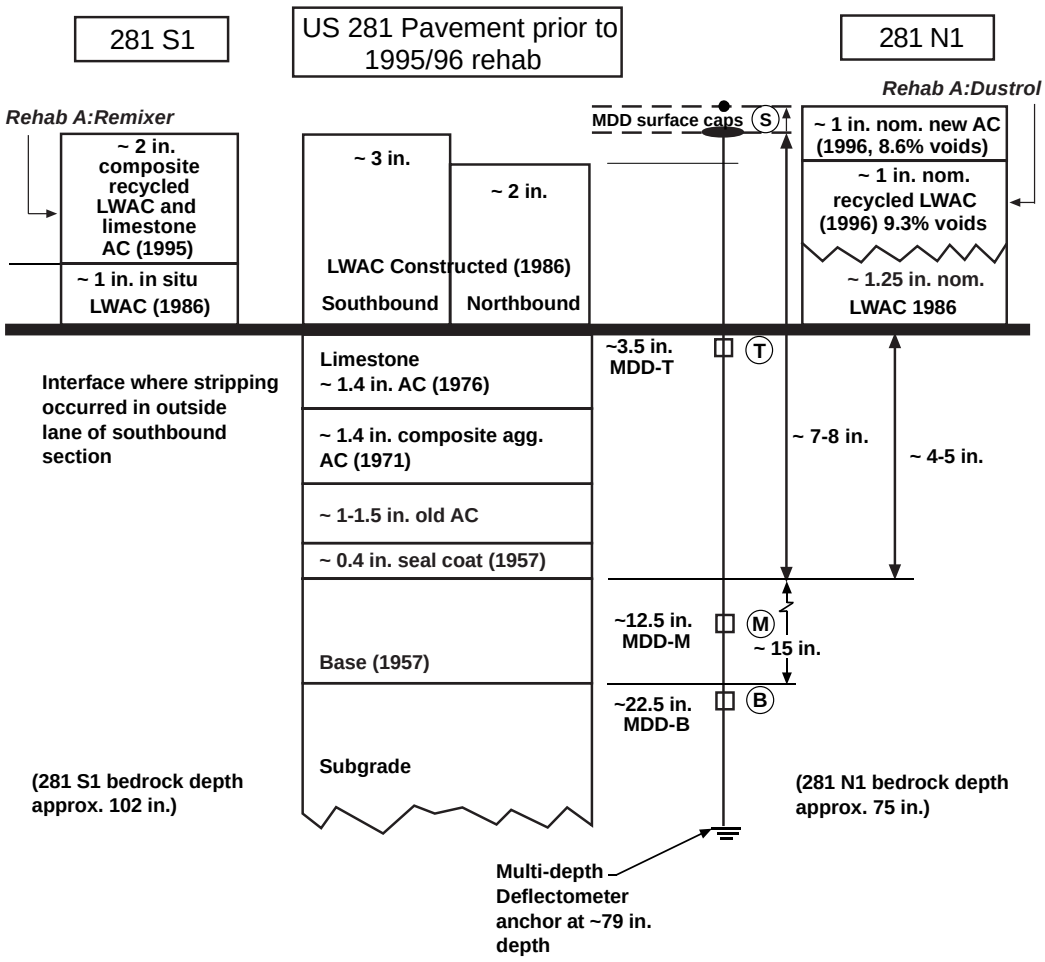

Figure 2 Pavement Sections of US 281

The recycling strategy used for the southbound lanes involved reworking the top 2 in. of the existing LWAC surface layer. It was milled, and some fresh material was added. Thereafter it was remixed and relaid in a single operation. The recycling strategy used for the northbound lanes included a reworking of the top 1 in. of the existing LWAC with the addition of a rejuvenator (Reclamite), followed by a 1 in. limestone AC overlay. The difference in rehab methods resulted in a slightly thinner AC on the southbound lanes than on the northbound lanes, as shown in Figure 2.

The inside southbound lane of US 281 was closed to traffic in April of 1997 while the outside lane remained open. Testing commenced on May 13, 1997. At that time, Nuclear Density Gauge (NDG) testing was conducted to measure the in situ AC density of test pad 281 S1. The average density was 117 pcf. This low value is a result of the significant amount of lightweight aggregate in the AC layers. For the top, 2-in., remixed layer, approximately 12 to 13 percent of air voids were found under the nontrafficked area, and 5.4 percent were found under the trafficked area.

The GPR data and construction record indicated that the test sections were situated on shallow bedrock. An auger and an extended Dynamic Cone Penetrometer (DCP) were used to measure the depth to bedrock, which was found to be at an average depth of 103 in.

The pavement structure of 281 N1 is very similar to that of 281 S1. The averaged NDG test results on the northbound section indicated that the density was 127 pcf. The testing on the northbound lane commenced on June 11, 1998. The depth to bedrock was found to be at an average depth of 75 in. on the north side.

The dimensions of the test pads were approximately 10 ft wide by 40 ft long (or 3 m by 12 m), as shown in Figure 3. This figure also shows the test section with transverse profiles, FWD, Multiple-Depth Deflectometer (MDD), and DCP locations. Test locations were the same for PSPA and FWD and were collected at 1.5 m (≈5 ft) intervals along the test section.

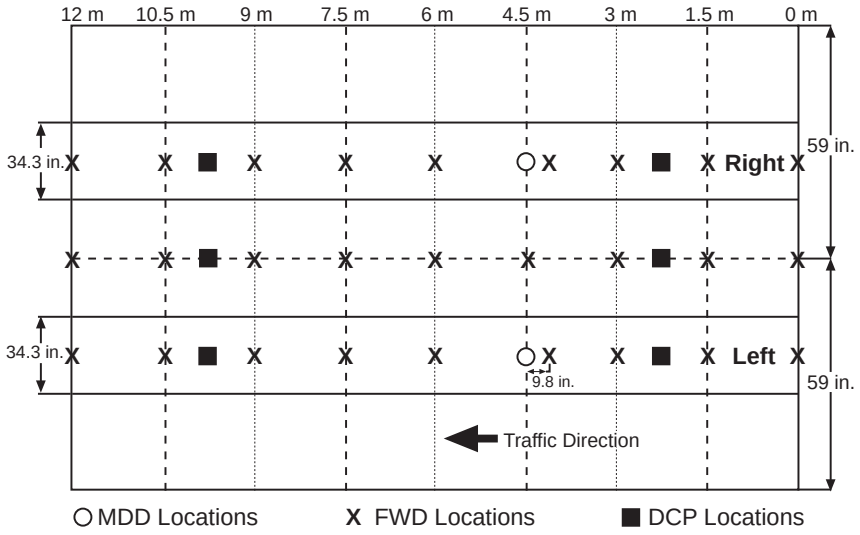

Note: Gridlines set out at 1.5 m (~5 ft) intervals. (1 m = 3.28 ft)

Figure 3 Test Section with FWD, Multi-Depth Deflectometer (MDD), and DCP Locations

TEST STRATEGY

The following factors were taken into account when planning the test program for MLS trafficking:

- Because the two test sections were tested at different times, each test section was subject to different rainfall events and dry seasons. Moisture content in the subsurface layers could also change in each test section. The variation of moisture content could influence the effectiveness of the rehabilitation processes.

- The pavement performance depends on the type of load to which the pavement is subjected and the way the load is applied. It was important to determine the difference in wander patterns between the MLS and conventional traffic.

- The test section was constantly covered by the MLS. It was important to measure the difference in pavement temperature inside and outside the MLS.

- Since some of the failures in rehabilitation projects are caused by the subsurface layer (and not the rehabilitation process itself), it was imperative to detect the source of the distress.

Several measures were taken to prevent incorrect judgment of the rehab processes:

(1) Time Domain Reflectometers (TDRs) were installed in the base and subgrade to monitor the subsurface moisture movement.

(2) Thermocouple trees were installed at various depths of the asphalt layer to measure pavement temperatures. The trees were embedded in the pavement both inside and outside of the MLS to determine the temperature differences.

(3) Multi-Depth Deflectometers (MDD) were installed to measure layer elastic deflections and permanent deformation. Linear Variable Displacement Transducers (LVDTs) were located in the asphalt, base, and subgrade layers to measure transient deflections and permanent deformation.

(4) A highway section with visible surface rutting was surveyed for comparison with the rutting from the MLS. This highway section was located 5 miles north of the MLS test site.

Test pad S2 (southbound) was tested with the TxMLS overloaded by 25 percent. Trafficking was limited (200,000 axle loads) and the results were inconclusive. Trafficking was interrupted after 200,000 axle loads for major mechanical repairs to the TxMLS. The test was terminated as inconclusive because the level of distress was small and virtually indistinguishable. In the same vein, the tires were overinflated to 120 psi to test the effect of tire pressure on the performance of test pad N2 (northbound). The findings of this test will be provided in TxDOT Report 1814-4 and in the summary report.

The water susceptibility and effect of high temperature trafficking were then investigated with the use of the third-scale Model Mobile Load Simulator (MMLS3). The tests and results are presented in TxDOT Reports 1814-2 and 1814-3.

Test Measurements and Surveillance

Response and performance of the test sections and material characteristics were measured and evaluated through the following:

- Falling Weight Deflectometer (FWD)
- Elastic Transient Deflection through Multi-Depth Deflectometer (MDD)
- Spectral Analysis of Surface Waves (SASW)
- Portable Seismic Pavement Analyzer (PSPA)
- Full-Depth Seismic Pavement Analyzer (SPA)
- Layer Rutting through MDD
- Cracking (patterns and extent)
- Transverse and Longitudinal Profiles, Quasi: PSI Index
- Dynamic Cone Penetrometer (DCP)
- Ground Penetrating Radar (GPR)

Laboratory tests were performed to characterize the material properties. Full details of the material characteristics are contained in Reports 1814-2 and 1814-3. The Hamburg wheel-tracking device was used to evaluate the rutting potential of both lanes of US 281. Repetitive triaxial and volumetric analysis (void, gradation, specific gravity, etc.) tests were also conducted.

FWD DATA PRIOR TO TRAFFICKING

FWD measurements were taken prior to testing to characterize the pavement condition.

Test Pad 281 S1

Three FWD tests were conducted at each of the 1.5 m (≈5-ft) grid intervals. There are twenty-seven FWD test locations, as shown in Figure 4. Because load level and temperature affect the FWD W1 (deflection at the center of the load) reading significantly, the deflections were normalized to 9,000 lb and 77 ^{o}F. Adoption of the temperature correction factors will be discussed later. The mean of fully normalized W1 deflections prior to trafficking was 12.4 mils, with a standard deviation of 3 mils, which yielded a 24 percent coefficient of variation (COV), as shown in Figure 4. The comparisons of 281 S1 and 281 N1 are based on the results from 3 m to 9 m grid lines only. For this range, W1=10.6 and the COV was found to be 5.85 percent.

Note that there are two visible surface transverse cracks near the 0 m and 10.5 m lines. These are believed to be caused by thermal effects. Figure 4 shows that the deflections are 60 percent greater at the 0 m and 10.5 m lines. The greater deflections here lead to a higher coefficient of variation. This is one reason it was decided that only the grid lines from 3 m to 9 m should be compared. The effects of axle load on FWD deflections are discussed later. No shrinkage cracks were observed prior to November 1996.

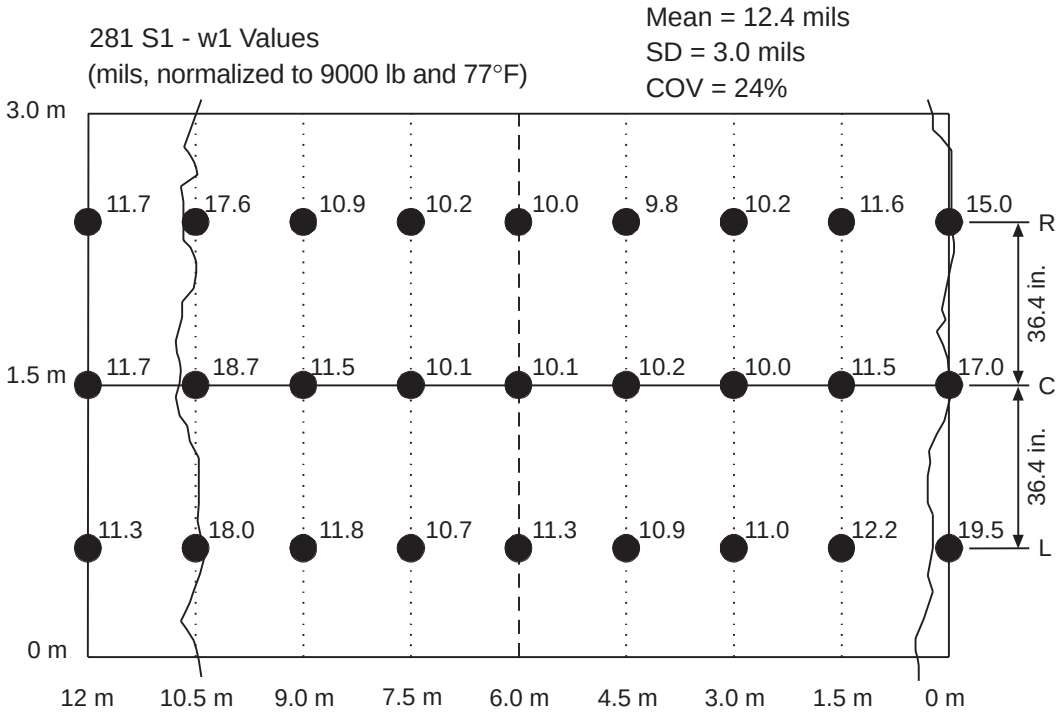

Note: 1 m = 3.28 ft

Figure 4 Surface Deflections (w1, at the center of the load plate) prior to MLS Trafficking for 281 S1

Test Pad 281 N1

There were also existing thermal cracks on 281 N1 in the vicinity of the 1.5 m and 12 m lines, as shown in Figure 5. The FWD W1 data here were also fully normalized to load and temperature. The mean, standard deviation, and COV values were 14.06 mils, 1.65 mils, and 12 percent, respectively. The COV was 12.96 percent for the results from the 3 m to 9 m grid lines. The deflection values from 281 N1 were consistently higher than those from 281 S1, but the variance was smaller. The PSPA results, which are presented later in this report, also indicate that the pavement of 281 N1 is generally weaker than that of 281 S1.

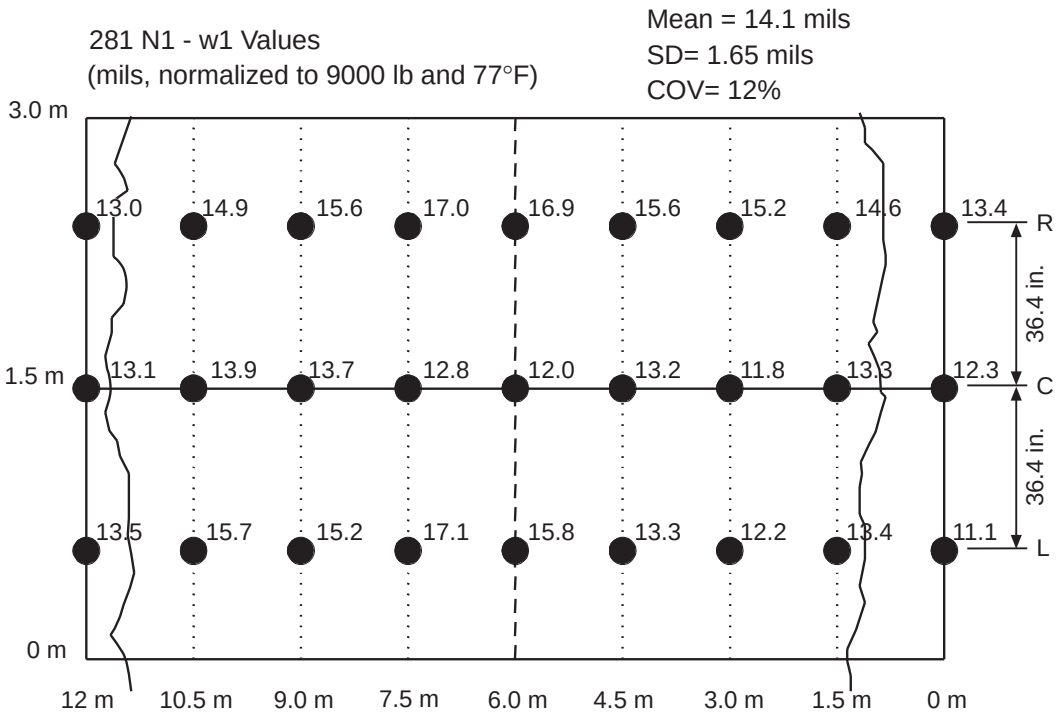

Note: 1 m = 3.28 ft

Figure 5 Surface Deflections (w1, at the center of the load plate) Prior to MLS Trafficking for 281 N1

MLS AXLE LOADING AND OPERATIONS

Captel Scales

Captel Weigh-in-Motion scales were used to measure and calibrate the axle loads applied by the MLS. Normally the intent is to have the wheel loads in the two wheel paths the same to within +/- 1 %. Even then, it is important to know the loads as accurately as possible, since the effect on distress is exponential! The loads were measured before and after each predetermined set of axle applications. The "before" and "after" readings are averaged and given in Figures 6 and 7 for 281 S1 and 281 N1, respectively. As shown in Figure 7 (281 N1), the right wheel path received loads 3 to 6 percent higher than those in the left wheel path in many instances.

Lateral Placement of Axle Tires and MLS Loading

Traffic loading plays a major role in pavement design and performance and in the evaluation process. Among other factors, the frequency distribution of truck wheel placement within the traffic lane determines the extent of pavement distress. The lateral offset of axle tires for the Jacksboro test site is presented in Figure 8. The same configuration was used for both

southbound and northbound lanes. The MLS consists of six tandem axles, for a total of twelve axles. The current configuration covers a wheel path width of approximately 34 in., which is the maximum width to which the MLS can be set.

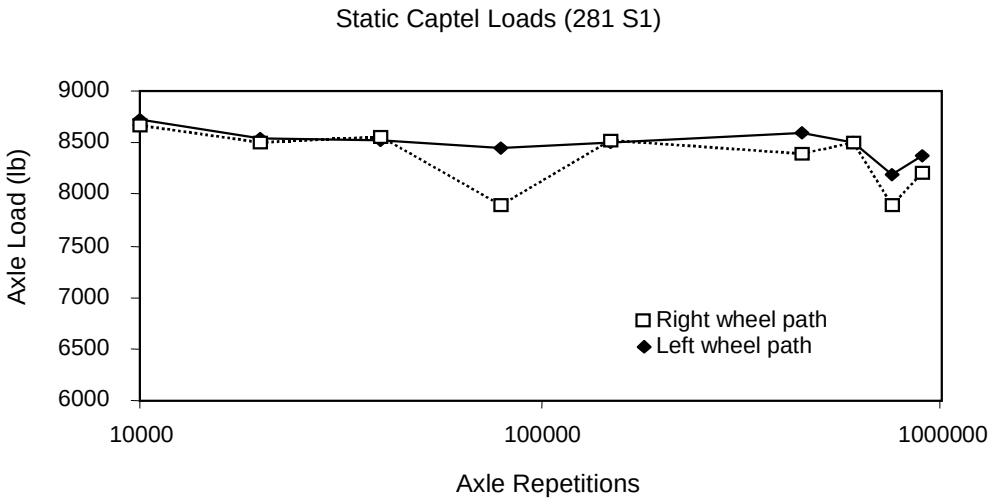

Figure 6 Axle Load Measured from Scales for 281 S1

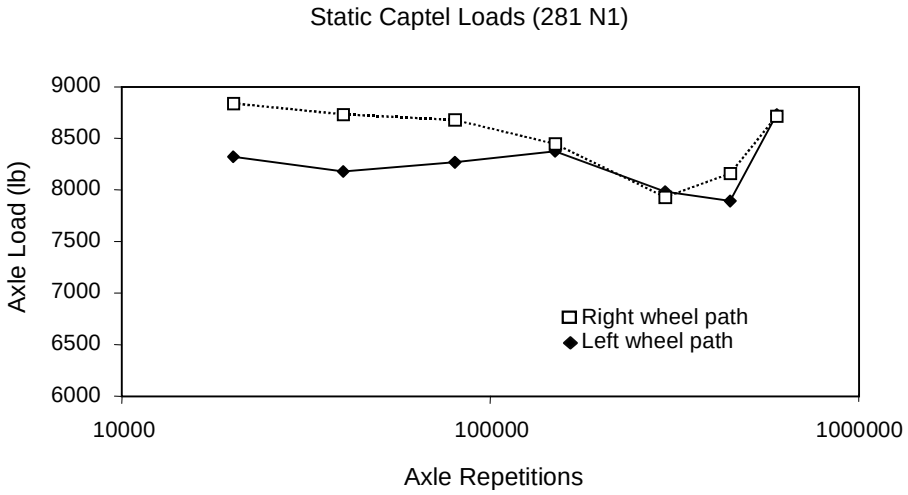

Figure 7 Axle Load Measured from Scales for 281 N1

According to field observations, the lateral wander for each wheel path may exceed 34 in. (Lee et al. 1983; Lee and Pangburn 1996). Figure 9 demonstrates the percentage covered at each point across the wheel path. The frequency distributions of truck wheel placements in a lane varies, depending on the type of truck, number of lanes, and location of the section (e.g., straight or curved roadway) (Lee et al. 1983). In Figure 9, the maximum percentage covered for the current study is 83 percent within a 3.9 in. wide section, while the majority of the section

(15.9 in.) is covered by 67 percent of the traffic. The calculation was based on a 9 in. wide tire and 3.9 in. spacing between dual tires, which were measured from the MLS. The width of the wheel path for the CAL/APT project is 39.4 in., which is the width of the test section (Metcalf 1996). CAL/APT selected the normal distribution as its wander pattern. The MLS test pads therefore received a higher frequency of axle loads than the CAL/APT sections.

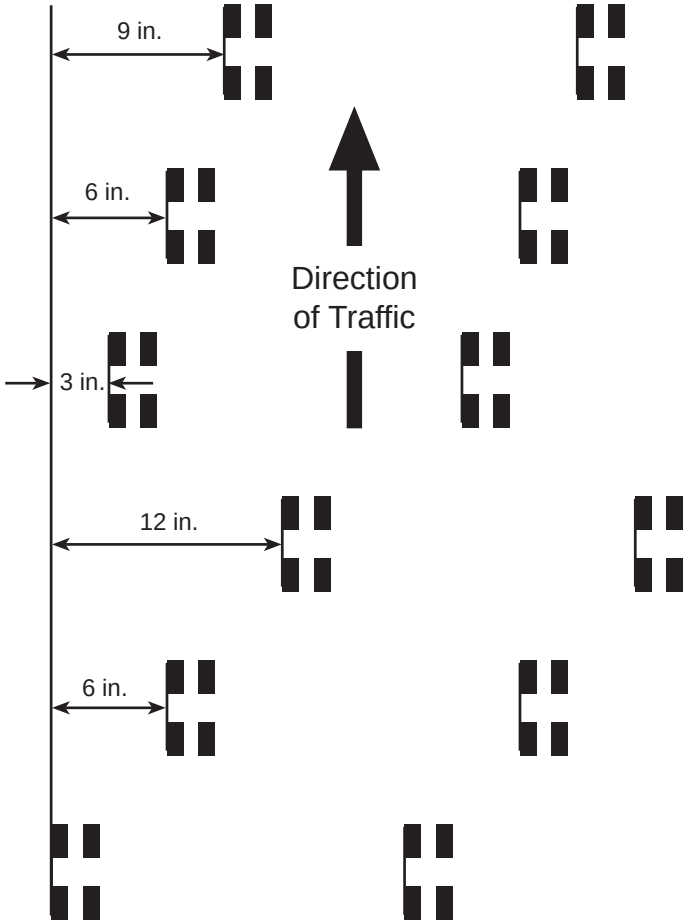

Figure 8 Offset of Six Tandem Axles

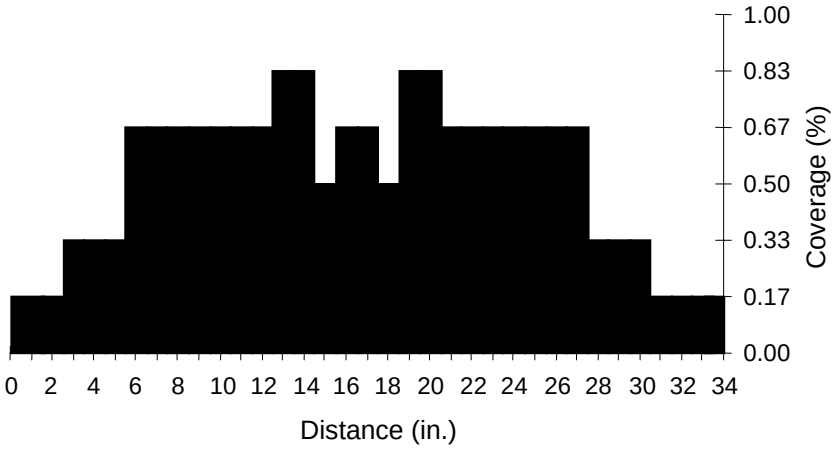

Figure 9 Traffic Distribution for Each Wheel Path

The lateral wander pattern determines the number of loads that will strike a particular location. The wider the wheel path, the lower the load intensity for a given point on the pavement. An effort was made to determine the difference in wander width between normal traffic and the MLS. A pavement section with visible surface rutting approximately 5 miles north of the MLS test site was selected. Two test grids, similar to those under the MLS, were laid out on the outside and inside lanes, as shown in Figure 10. Nine transverse profiles were collected for both the outside and inside lanes.

The widths of wheel wander were different for the inside and outside lanes. Wheel path widths of 53 in. (O1) and 35 in. (O2) were measured for the outside lane. Wheel path widths were 49 in. (I1) and 41 in. (I2) for the inside lane. Figure 11 shows this graphically. The wheel paths close to the shoulder are wider on both outside and inside lanes. In particular, wheel path O1 is the widest. The rut depth of O1 is the deepest because the road crown causes heavier loads to fall on the outside wheel path. A wider part of this wheel path is then considered "rutted." This shows how the same trafficking can generate two apparently different wheel path widths. In fact, a similar phenomenon was observed by the Project Director, Dr. Mike Murphy, on the SPS-1 site on US 281 in the Pharr District.

The comparison of transverse profiles between conventional traffic and the MLS is also presented in Figure 11. It is clear that the wheel paths of normal vehicle traffic are wider than those of the MLS. The average wheel path for the selected pavement section was 43.3 in. wide.

The MLS applies 67 percent of traffic over most (22 in.) of the wheel path, with a peak of 83 percent near the center. Thus, because of its higher concentration, the MLS may induce more damage per axle than conventional traffic.

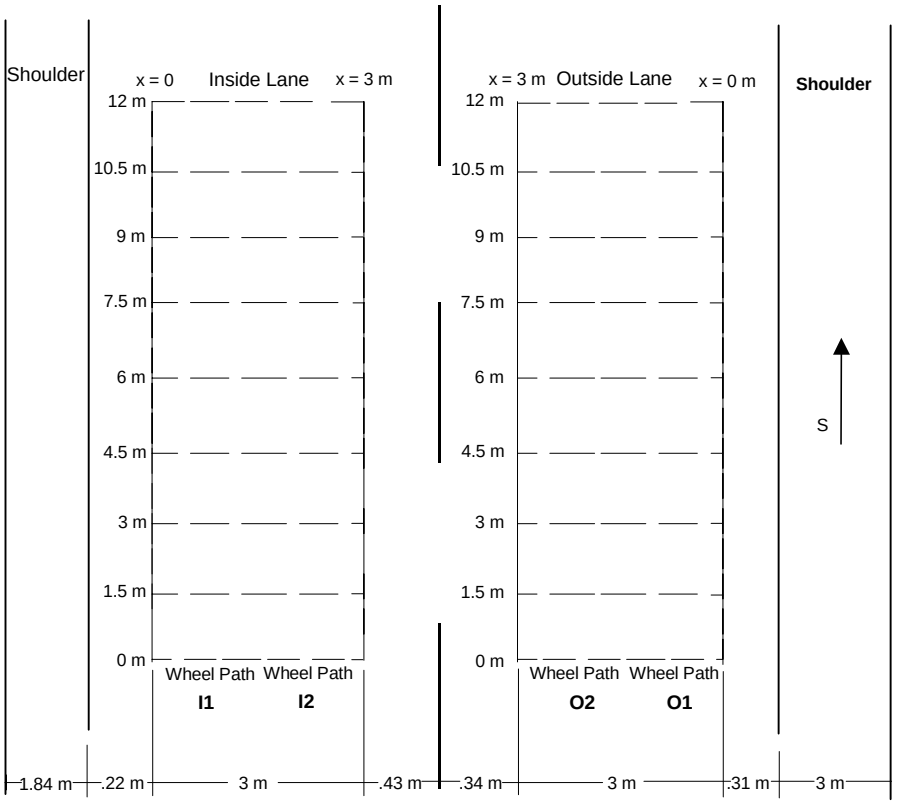

Note: 1 m = 3.28 ft

Figure 10 Transverse Profile Collection from an In-Service Pavement 5 Miles North of the MLS Test Sites

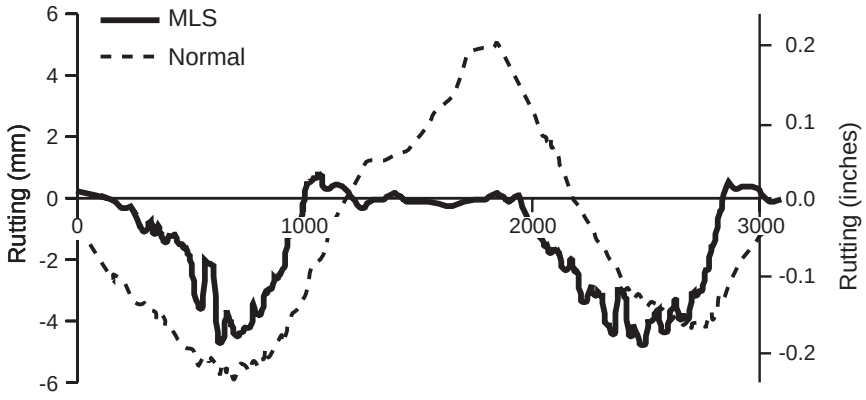

Figure 11 Comparison of Transverse Profile between Normal Traffic and the MLS

PAVEMENT-RELATED TEMPERATURE VARIATION AND SUBSURFACE MOISTURE MOVEMENT

The actual pavement temperature and moisture content need to be considered in the evaluation of the relative performance of the two pavements.

Thermocouples

Temperature probes were installed at three different depths within the AC layer: 0.5 in., 3.5 in., and 6.5 in. from the surface. Pavement and air temperature data were collected both inside and outside the MLS to determine temperature variation. On a typical sunny day, the most variation occurred at the 0.5 in. depth, which was typically 31 °F hotter outside than inside the MLS at noon. At the 3.5 in. depth, a 13 °F difference was observed, as shown in Figure 12 below. On overcast or rainy days, a less than 4 °F difference was observed at all three depths. Higher temperature variations occurred outside than inside the MLS, as expected. At the depth of 0.5 in., daily temperature variations (high minus low) of 20 °F and 50 °F were found inside and outside the MLS, respectively. For mid-depth temperature (3.5 in.) the temperature variation decreases. Shade, whether from the MLS or clouds, greatly decreases the range of pavement temperature. Shade also tends to increase the lag time between maximum air temperature and maximum pavement temperature. The pavement temperature outside the MLS at 0.5 in. depth experienced almost no time lag on a sunny day. However, it took the pavement inside the MLS and at the same depth 3 hours to respond to an increase in air temperature.

The MLS structural shell cover consistently reduces the daily temperature swing by 50 percent. Without the MLS cover, the daytime highs are higher (owing to sunlight) and the nighttime lows are lower (no wind protection). This tendency, most noticeable in the top 0.5 in. of AC, holds throughout the summer and winter months. At a depth of 6.5 in. into the AC layer under MLS cover, the day/night temperature change was found to be insignificant.

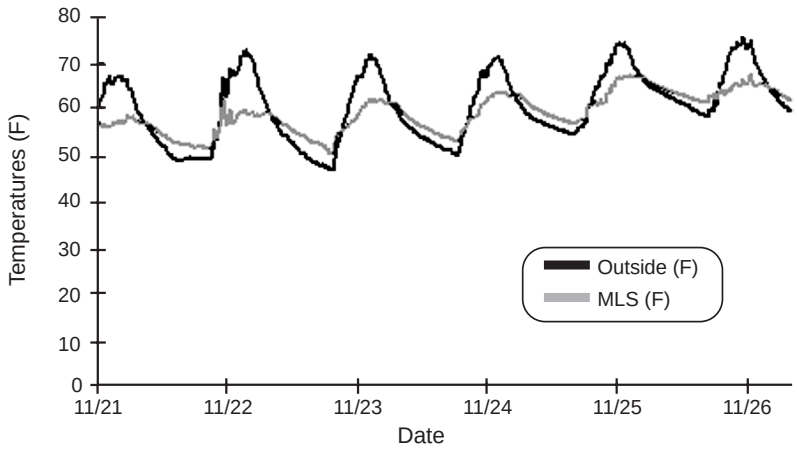

Figure 12 Temperature Variations at the Mid-Depth AC

The mean mid-depth pavement temperature variations during MLS trafficking are shown in Figures 13 and 14, together with the cumulative axles applied to 281 S1 and 281 N1, respectively. Because of several breakdowns of the weather station, there are gaps in the data. The average mid-depth pavement temperatures up to 600,000 axle repetitions were 81 °F and 88 °F for 281 S1 and 281 N1, respectively. The average mid-depth pavement temperature up to 1.5 million axle repetitions for 281 S1 was 80 °F. It is important to note that the average air temperatures during the tests were 82 °F (281 S1) and 89 °F (281 N1), respectively.

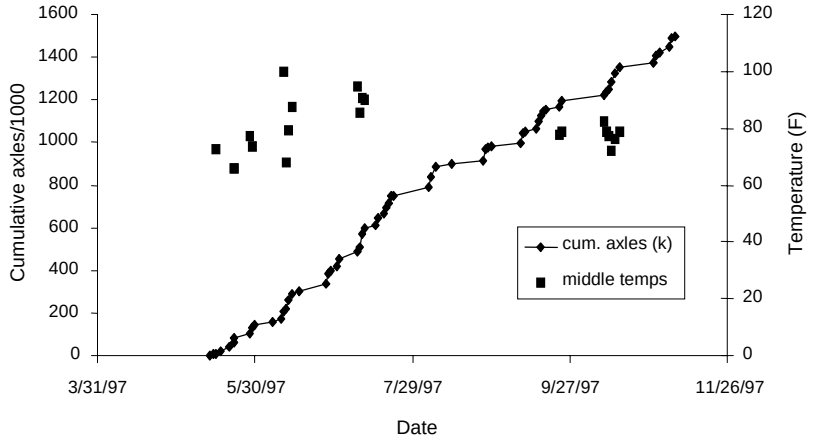

Figure 13 Mean Daily Mid-Depth Pavement Temperature Variation during Trafficking for 281 S1

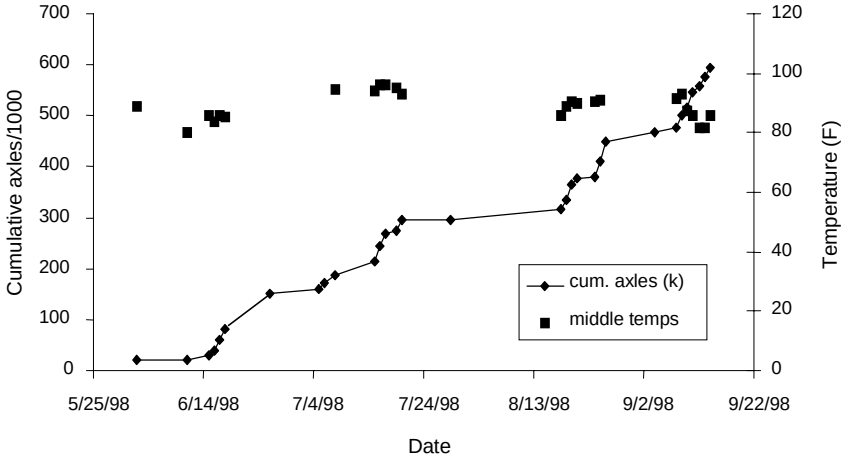

Figure 14 Mean Daily Mid-Depth Pavement Temperature Variation during Trafficking for 281 N1

Time Domain Reflectometer (TDR)

Soil moisture content can be determined by the effective dielectric constant of the soil, because the dielectric of liquid water is at least 15 times greater than the dielectric of common soil constituents. The effective dielectric constant can be measured using a Time Domain Reflectometer (TDR). Eight TDRs were embedded in the pavement—two at the mid-depth of the base, three at a nominal 6 in. into the subgrade, and three at 18 in. into the subgrade, as shown in Figure 15. There were three holes to accommodate these eight TDRs. Three TDRs were located below the center of each wheel path, and two were located below the shoulder. After the TDRs were installed, the holes were back-filled with the original subgrade and base and then with cold-mix AC to replace the original AC. TDR readings from under the surface-treated shoulder were used as references because they were more sensitive to rainfall events. Measurements were taken for both S1 and N1.

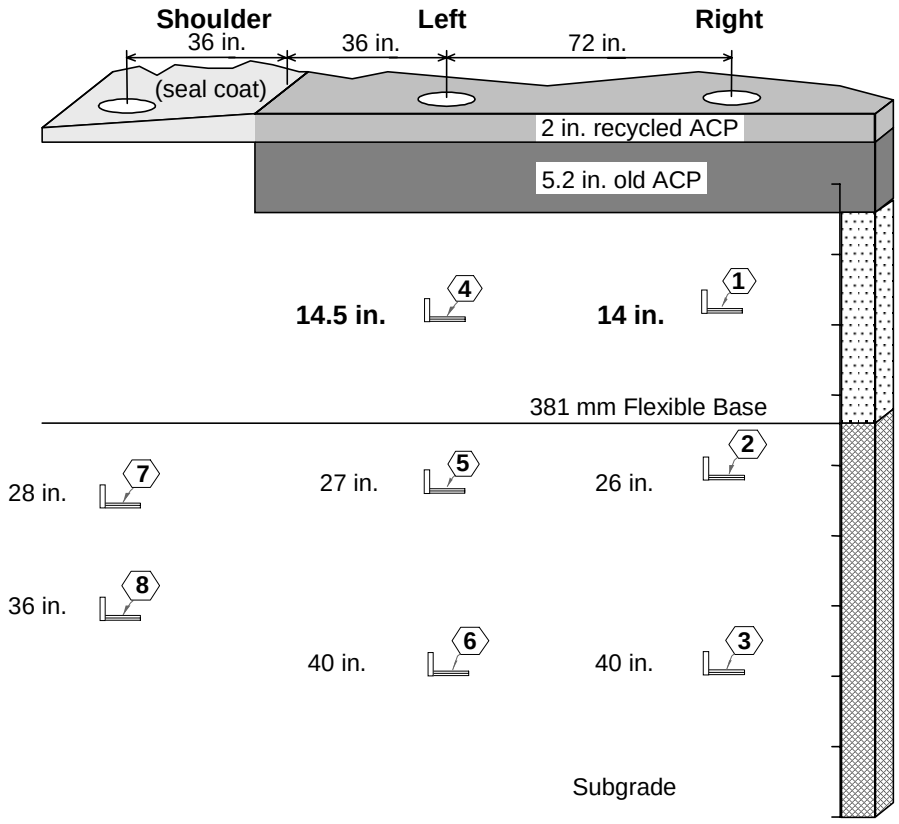

Figure 15 TDR Locations for Southbound US 281

An effort was made to investigate the pavement drainage system and to compare it to those recommended by the American Association of Highway and Transportation Officials (AASHTO) pavement design handbook. AASHTO recommends the time-to-drain concept. If

the pavement system takes less than 2 hours to drain 50 percent of drainable water, the drainage system is considered "excellent." Similarly, the quality of the drainage system is "good" when the system needs 24 hours to drain 50 percent of all drainable water. The time to drain is measured from the time the medium is fully saturated. Thus, an event with significant rainfall to bring the base to a fully saturated condition was selected. The accumulated rainfall was 0.75 in., and the duration was about 4 hours, as shown in Figure 16. After the moisture content had reached its peak, the time to drain 50 percent of the moisture gained was found to be 4.5 hours. The same pavement section took 16 hours to drain 90 percent of the moisture gained. Therefore, the test section has a fairly good drainage system.

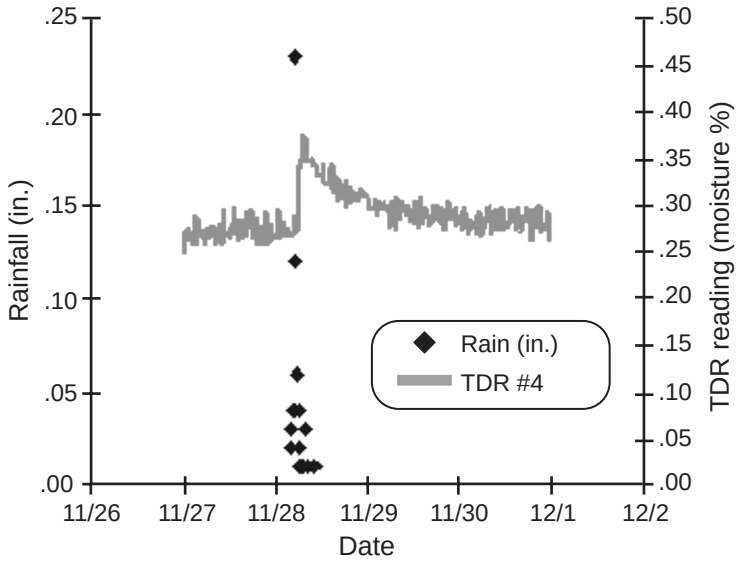

Figure 16 Moisture Movement in the Mid-Depth of the Base Layer

RESPONSE DATA AND ANALYSIS

In order to gain insight into the relative performance of the two pavements, the response data were reviewed and analyzed.

NORMALIZATION OF FWD RESULTS FOR TEMPERATURE EFFECTS

To determine an appropriate temperature conversion model, Dr. Chen and his TxDOT staff conducted repeated FWD tests in the vicinity of the 281 S1 and 281 N1 test pads. No traffic load was allowed during the period of repeated FWD testing. Thus, it is reasonable to assume that once these FWD deflections are normalized to a specific load, any variation is due to environmental conditions. Repeated FWD tests were conducted at regular intervals for 2 to 3 consecutive days at the same location. This was done in the months of February, May, and August to obtain the widest possible range of temperatures. Figures 17A and 17B show that only the W1 and W2 deflections are influenced by mid-depth pavement temperature. Linear

regression was used to correlate maximum FWD deflection to pavement temperature. The temperature correction factors were established by Dr. Chen from his field studies. His findings are shown in Equations 1 through 4. FWD deflections were normalized to a temperature of 77 °F. The temperature correction factors for the maximum FWD deflection (W1) of 281 S1 and 281 N1 are presented in Figures 18A and 18B, respectively. It is not readily apparent why the corrections factors differ for the two pavements that are so much alike, the only real difference being the nature of the rehabilitation surface layers.

Test Pad US 281 S1

$$W_{77}^{1} = W_{Tc}^{1} * [-0.0107 * T_c + 1.807] \quad \text{(Eq 1)}$$

$R^2 = 0.9717$

$$W_{77}^{2} = W_{Tc}^{2} * [-0.00622 * T_c + 1.476] \quad \text{(Eq 2)}$$

$R^2 = 0.9515$

Where

T_c = mid-depth pavement temperature at the time of FWD data collection, ^{o}F

W_{77}^{1} = the adjusted W1 deflection to 77 ^{o}F, mils

W_{Tc}^{1} = the measured W1 deflection at T_c, mils

W_{77}^{2} = the adjusted W2 deflection to 77 ^{o}F, mils

W_{Tc}^{2} = the measured W2 deflection at T_c, mils

Test Pad US 281 N1

$$W_{77}^{1} = W_{Tc}^{1} * [-0.0141 * T_c + 2.161] \quad \text{(Eq 3)}$$

$R^2 = 0.9822$

$$W_{77}^{2} = W_{Tc}^{2} * [-0.00544 * T_c + 1.430] \quad \text{(Eq 4)}$$

$R^2 = 0.9486$

Where T_c, W_{77}^{1}, and W_{77}^{2} carry the same meaning as they do in Equations 3 and 4.

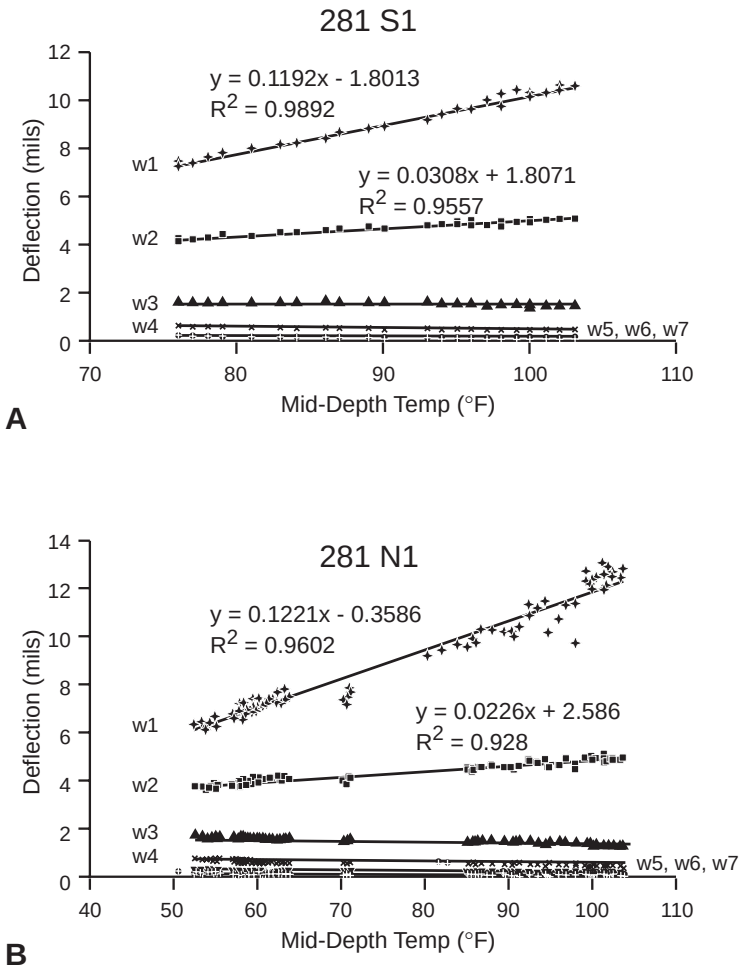

Figure 17 Temperature Influence on FWD Deflections, (A) 281 S1 and (B) 281 N1

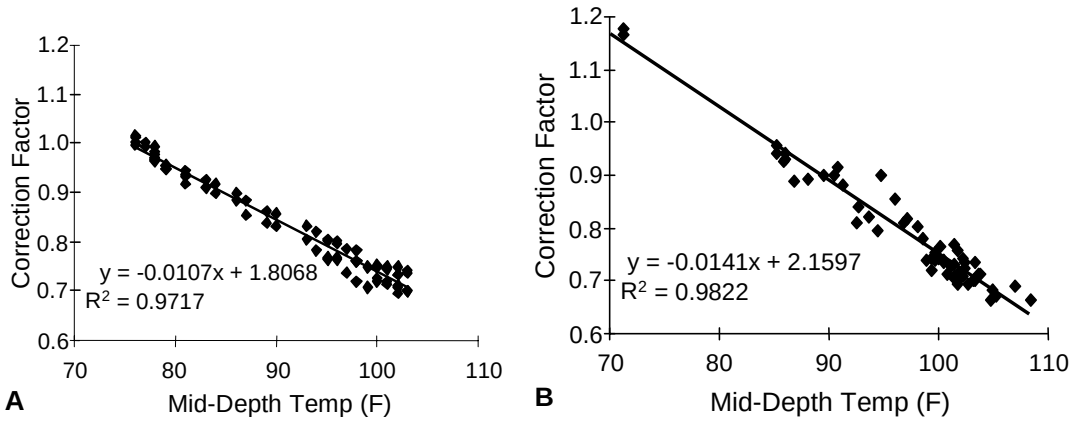

Figure 18 Temperature Correction Factor (Normalized to 77°F), (A) 281 S1 and (B) 281 N1

FALLING WEIGHT DEFLECTOMETER (FWD)

FWD data were collected for test pad 281 S1 prior to testing and after axle repetitions of 2.5 k, 5 k, 20 k, 40 k, 80 k, 160 k, 300 k, 450 k, 600 k, 750 k, 900 k, 1,050 k, 1,200 k, 1,350 k, and 1.5 million. After 160 k axle repetitions, the increment of 150 k was selected because it ties in with the weekly production rate of about 150 k repetitions. Because no significant variation was observed at the early stages of trafficking (and in order to increase the production rate), the data collection intervals for 281 N1 were reduced to those used prior to trafficking and after 20 k, 40 k, 80 k, 150 k, 300 k, 450 k, 600 k, and 750 k axle repetitions.

FWD Deflections on the Cracked Section

One interesting phenomenon was that, because of a nearby surface crack, the W1 deflection for the 10.5 m line of pad 281 S1 was approximately 60 percent greater than that for the rest of the pad. The deflection basin at the 10.5 m line differed from those in the areas without any cracking. The comparisons of deflection basins at the 10.5 m, 3 m, and 9 m lines are given in Figures 19A, 19B, 19C, and 19D after 0 k, 80 k, 750 k, and 1,500 k axle repetitions, respectively. The deflections in Figure 19 were first normalized to a 9,000 lb load. Then W1 and W2 were normalized to 77 ^{o}F using Equations 1 and 2. Because the temperature had no effect on the W3 to W7 readings, these readings were not normalized. The W1 (at the center of the load) and W2 (12 in. from the center of the load) surface deflections were much higher at 10.5 m than those at 3 m and 9 m. However, the rest of the surface deflections (from W3 to W7) were of similar magnitude at the same lines. Thus, the surface crack mainly caused an increase in deflections W1 and W2. A diagnostic investigation (coring after trafficking) showed that the cracks extended through the AC layer. It can be observed in Figure 19 that traffic load caused more deterioration at 10.5 m near the crack.

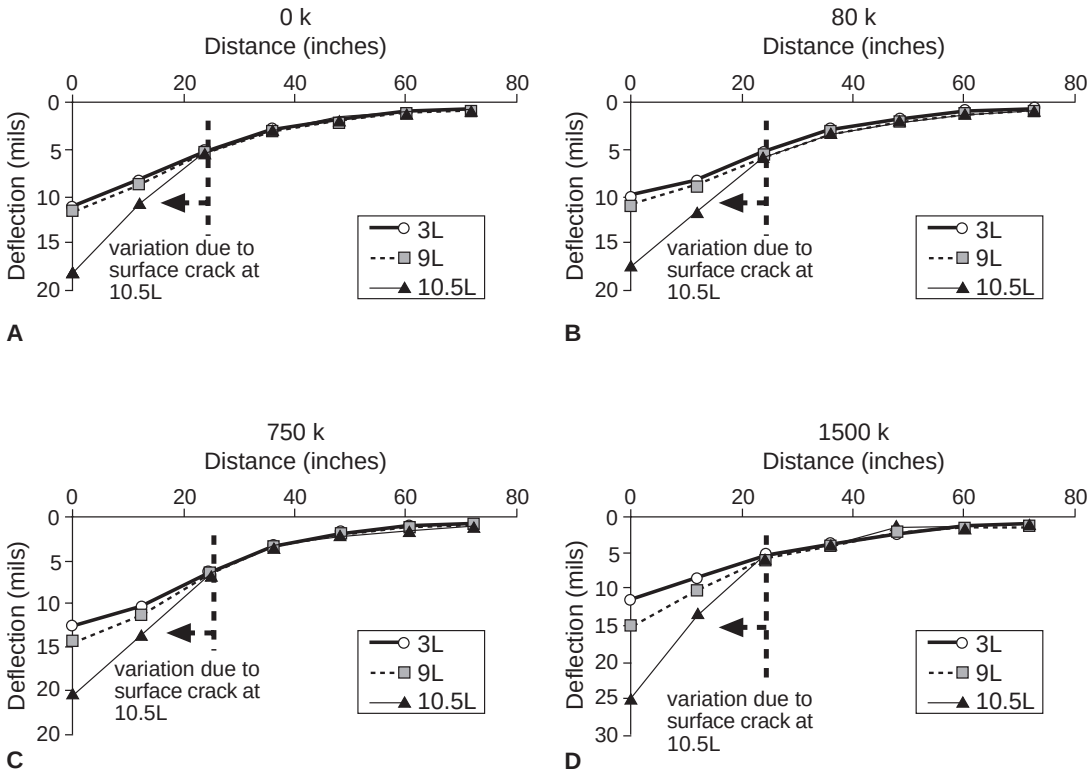

Figure 19 Comparison of Deflection Profiles between Cracks and No-Cracks Locations at Various Axle Repetitions, (A) 0, (B) 80,000, (C) 750,000, and (D) 1,500,000

Variation of FWD Deflections for Test Pad US 281 S1

Figures 20A and 20B show fully normalized FWD deflections in the left and right wheel paths (and along the centerline) at the 14.85 ft and 19.9 ft (4.5 m and 6 m) grid lines with respect to MLS trafficking. It is apparent that the deflections along the centerline of the test pad do not change significantly during the trafficking tests. The location of the centerline (C) is shown in Figure 4. The centerline is never under any load from the MLS. The fact that there were no significant changes in deflections suggests that the material properties in this region did not change with trafficking. This phenomenon has been reported previously (Chen and Hugo [1998] and Yuan et al. [1998]).

Because there were cracks at the 0 and 34.65 ft (0 m and 10.5 m) lines, the average FWD deflections between 9.9 ft and 29.7 ft (3 m and 9 m) were used to represent the whole test pad. These deflections are shown in Figure 20A. As expected, there was no significant difference between the two wheel paths. However, rutting was slightly higher in the right wheel path than in the left, as will be shown later.

After 1.5 million axle repetitions, deflections in the wheel paths had increased approximately 40 percent at 14.85 ft (4.5 m), 36 percent at 19.9 ft (6 m), and 38 percent for the 9.9 ft and 29.7 ft (3 m and 9 m) average.

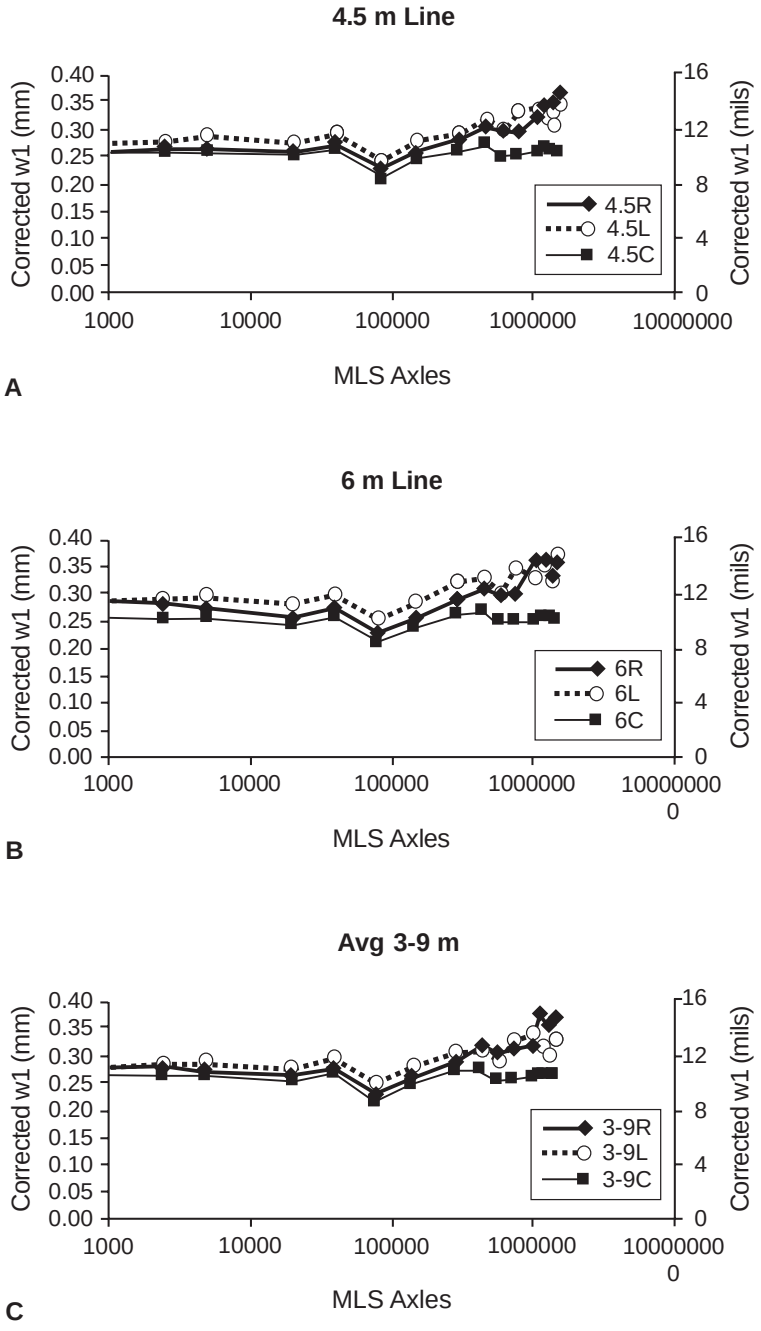

Note: 1 m = 3.28 ft. 1 mm=0.04 in.

Figure 20 W1 Deflections vs. Axle Repetitions for 281 S1, (A) 4.5 m Grid Line, (B) 6 m Grid Line, and (C) Average from 3 m to 9 m Grid Lines

Variation of FWD Deflections for Test Pad US 281 N1

The normalized FWD deflections at the 14.85 ft and 19.9 ft (4.5 m and 6 m) grid lines, and the averaged deflections from the 9.9 ft to 29.7 ft (3 m to 9 m) lines are given in Figures 21A, 21B, and 21C. As expected, deflections along the centerline remained almost constant. After 600,000 axle repetitions, deflections in the wheel paths had increased approximately 32 percent at 14.85 (4.5 m), 19 percent at 19.8 ft (6 m), and 34 percent for the 9.9 ft to 29.7 ft (3 m to 9 m) average.

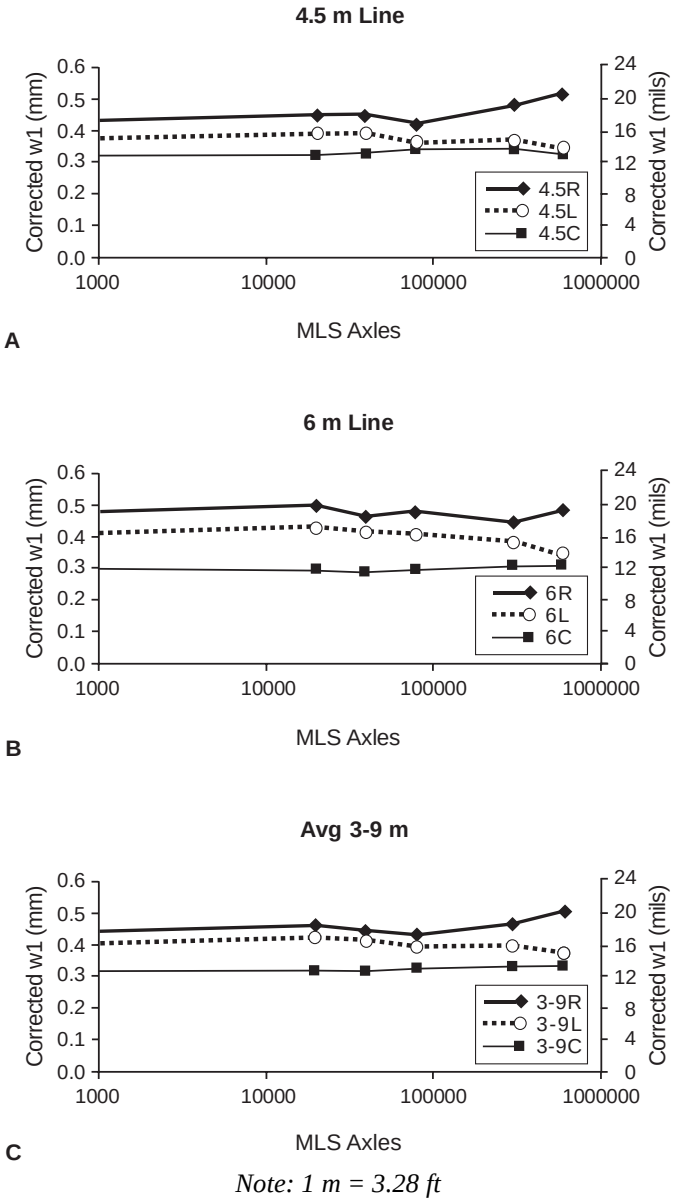

Note: 1 m = 3.28 ft

Figure 21 W1 Deflections vs. Axle Repetitions for 281 N1, (A) 4.5 m Grid Line, (B) 6 m Grid Line, and (C) Average from 3 m to 9 m Grid Lines

PSPA (PORTABLE SEISMIC PAVEMENT ANALYZER)

Seismic techniques were employed to measure the stiffness of the pavement layers through in situ nondestructive testing. The basis of the techniques is measurement of Raleigh-type surface waves. Their velocity (VR) is constant in an elastic, homogeneous half-space and independent of frequency (f). If the half-space varies with depth, the velocity of the Raleigh waves will vary with frequency. This variation of wave velocity with frequency, called *dispersion,* arises because waves of different wavelength (L_r) sample different portions of a layered medium. All layers can therefore be sampled by generating surface waves with different wavelengths (or frequencies). Estimates of Young's modulus can be determined from VR.

This information provides a valuable means of monitoring progressive changes in the pavement's structural stiffness owing to distress caused by trafficking or the environment. It has been shown that stiffnesses deduced by seismic techniques correlate well with those measured by other means, such as by resilient modulus and indirect tensile modulus (Nazarian et al. 1999; Yuan et al. 1998). Detailed information on PSPA equipment, operation, and analysis procedures can be found in Nazarian et al. (1999) and in Yuan et al. (1998). More complete PSPA test results on 281 N1 and 281 S1 were presented by Nazarian et al. (1999). Only comparisons of stiffness values before trafficking are considered here.

The average AC modulus of 281 S1 was approximately 20 percent higher than that of 281 N1. Both the upper and lower (top 2 in. and next 2 in.) AC layers of 281 S1 were stiffer than those of 281 N1 (Nazarian et al. 1999). Figure 22 shows a comparison of the dispersion curves from 281 S1 and 281 N1. The Raleigh wave velocities of 281 S1 were always higher than those of 281 N1 (from wavelength of 1.6 in. to 8 in.). In particular, the lower AC layer of 281 N1 exhibited a gradual reduction in phase (R) velocity with wavelength (or depth). By contrast, the velocity of the lower AC layers of 281 S1 was much lower.

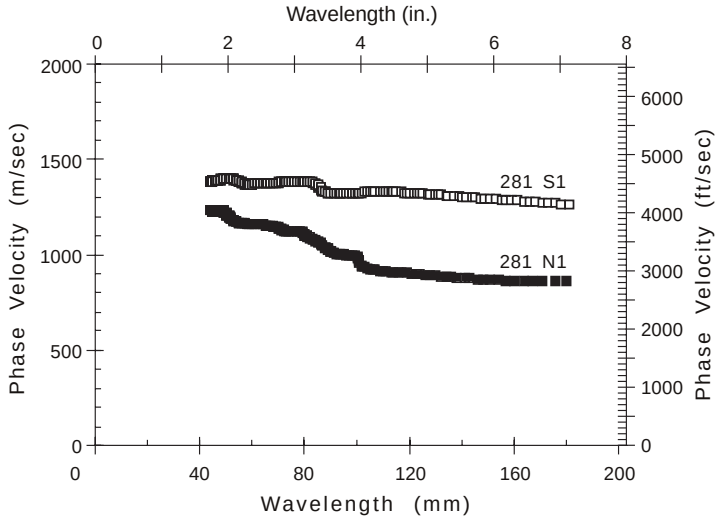

Note: 1 m = 39.4 in., 1 m/sec = 3.28 ft/sec

Figure 22 Comparison of Dispersion Curves of 281 S1 and 281 N1

ANALYSIS OF MULTI-DEPTH DEFLECTOMETER (MDD) RESULTS

Because the main objective of this research was to determine the comparative effectiveness and performance of two rehabilitation processes (Remixer and Dustrol), it was imperative that the researchers have instrumentation capable of identifying the layer properties under traffic loading. One of the most important elements of monitoring rutting performance is the quantification of each layer's contribution to rut depth. In some rehabilitation projects, failures of the overlay are caused by the subsurface layer(s) and not by the overlay itself. With this in mind, the researchers installed two MDDs for every MLS test site. In each MDD hole, three LVDTs were installed to measure deflections at three different depths, as shown in Figure 23. The Texas Transportation Institute installed the MDDs. MDDs revealed not only the transient responses under load, but also the accumulated permanent deformation. Ideally, an LVDT is placed at each layer interface, so that the deflection contribution of each layer can be measured directly. Because mechanical limitations made this impossible, the MDD sensors were installed as close as possible to the ideal depths. MDDt, MDDm, and MDDb are used to refer to the LVDTs at the depths of 3.5 in., 12.5 in., and 22.5 in., respectively. All three LVDTs were anchored at a depth of approximately 80 in. During the installation process, bedrock was encountered at a depth of 75 in. for test pad 281 N1. Figure 23 shows the MDD depths and their relation to the pavement layers for pads 281 S1 and 281 N1.

The surface rutting data were collected using a transverse profiler. A detailed description of the transverse profiler and data collection can be found in Chen and Hugo (1998). The surface rutting and layer rutting values presented in this study are averaged from both wheel paths.

One of the advantages of the MDD is its ability to measure the permanent deformation within the pavement structure. The permanent deformation recorded by the bottom LVDT (MDDb) is the subgrade contribution to rutting. The difference between MDDm and MDDb displacement is the rutting contributed by the bottom 10 in. of base material (see Figure 23A). Also, the difference between MDDt and MDDm displacement is the contribution of the bottom 3.7 in. of AC and top 5 in. of base. The rutting contributed by the top 3.5 in. of AC is the difference between surface rutting and permanent displacement recorded by the MDDt.

Because the LVDTs were not installed at each layer interface, assumptions had to be made in order to compute the rutting for each pavement layer. For the analysis, nominal values were used for the layer thicknesses. While many assumptions can be used to assist in the computation of layer thickness, only two were explored:

Assumption 1

The rutting from the bottom 10 in. of base is proportional to the top 5 in. of base. Thus, the rutting from the full 15 in. of base material was calculated by multiplying the 10 in. base rutting by 1.5 (or 1.5 x [MDDm – MDDb]), since that is the ratio of 15 in. to 10 in.

$$\text{Rutting}_{15\text{in base}} = 1.5\ (\text{MDDm} - \text{MDDb}) \qquad \text{(Eq 5)}$$

The lower AC rutting was then computed by prorating the measured base deformation, as in Equation 7. The factor of 0.5 in Equation 6 is the ratio of the top 5 in. to the measured bottom 10 in. of base.

$$\text{Rutting}_{\text{lower 3.7 in. AC}} = (\text{MDDt} - \text{MDDm}) - 0.5\,(\text{MDDm} - \text{MDDb}) \qquad \text{(Eq 6)}$$

For 281 N1, the factors of 1.5 in Equation 5 and 0.6 in Equation 6 need to be adjusted according to the pavement thickness.

Assumption 2

The rutting at the top of the base layer should occur at a higher rate than that at the bottom (because of the higher stress at the top). Thus, to compute the nonproportional base rutting, ELSYM5 was used with the assumption that the permanent deformation was proportional to the elastic deformation. The elastic deformations for the top 5 in. and bottom 10 in. of base were computed. Stress dependency of the flexible base was ignored in the analysis. The rate of the rutting was computed to be a factor of 1.8; that is, the rutting for a 15 in. base is equal to 1.8 of MDDm – MDDb (rutting from bottom 10 in. of base) for 281 N1. Because the stress is higher, the elastic deformation for the top 5 in. is higher than that for the bottom 10 in. of base. For 281 S1, the factor was 1.72. The factors of 1.8 and 1.72 are higher than the factor of 1.5 in Equation 6, as expected. Thus, the lower AC deformation of 281 N1 can be computed as in Equation 7.

$$\text{Rutting}_{\text{lower 3.7 in. AC}} = (\text{MDDt} - \text{MDDm}) - 0.8\,(\text{MDDm} - \text{MDDb}) \qquad \text{(Eq 7)}$$

For the lower AC of 281 S1, the factor of 0.8 in Equation 7 needs to be replaced with 0.72.

The results for surface and layer rutting were computed using Assumption 2; these results are presented in Table 2 and in Figure 24. The measured and percent rutting contributed by surface, base, and subgrade layers are also presented. Because the majority of the rutting for pads 281 S1 and 281 N1 was from the AC layer, the influence of using either Assumption 1 or 2 was less than 10 percent for both cases.

A more accurate calculation for this deformation could take into account the effect of stress dependency. (This has been explored and has been found to have no significant effect.)

The MDD data in Table 2 indicate that the majority of the rutting for pads 281 S1 and 281 N1 was from the AC layer, which contributed more than 70 percent. The top 3.5 in. of AC contributed approximately 69 percent and 51 percent of overall surface rutting for 281 S1 and 281 N1, respectively. The rutting in the top 3.5 in. of AC in 281 N1 was 2.6 times higher than it was in 281 S1, as shown in Table 3. The combination of the rutting of both the base and subgrade in 281 N1 was 4.9 times higher than it was in 281 S1. This mechanism can be explained by showing that the weaker asphalt layer in 281 N1 led to higher stress penetration into the base and subgrade and caused higher rutting in the subsurface layers. The base and subgrade layers contributed 22 percent and 31 percent of the overall rutting for 281 S1 and 281 N1, respectively. Because the subsurface layers had been in service since 1957, the low rate of rutting was to be expected, particularly because the rehab in both cases was still relatively fresh, having experienced limited trafficking prior to testing.

For test pad 281 N1 it is important to note that the results show trends similar to those for 281 S1, though the total deformation is greater by a factor of between 2 and 3 for the same axle count. This finding, a result of the different test temperature, different structural response,

and different characteristics of the asphalt (Hugo et al. 1999), is discussed in more detail later in the report.

The Hamburg Test

The Hamburg wheel-tracking device (HWTD) shown in Figure 25 has been used to evaluate the rutting and stripping potential of asphalt concrete since the 1980s (Aschenbrener et al. 1994). The HWTD used in this study was equipped with a steel wheel 8 in. in diameter and 1.9 in. wide. The wheel load was set to 158 lb and the wheel speed was 1.1 fps at the center of the sample. During the testing, specimens were submerged in water. The cores at the center of the inside lane (or fast lane) of both northbound and southbound lanes were used for the tests. Each Hamburg test required four specimens—two for each wheel path.

Subjecting specimens to 20,000 passes is the standard test procedure performed by TxDOT. Historical test data have shown that specimens yielding less than 0.16 in. after 20,000 passes are considered satisfactory mixes, as specified in Hamburg, Germany (Izzo and Tahmoressi 1999). Through its extensive use of the HWTD since 1990, the Colorado Department of Transportation (CDOT) developed a procedure to assess the potential of moisture damage of HMA in Colorado (Aschenbrener et al. 1994). The procedure specifies testing temperatures according to site location and asphalt binder type. A maximum allowable rut depth of 0.4 in. at 20,000 passes is specified by CDOT.

From the pilot tests, it was found that the specimens at the end of 20,000 passes yielded only approximately 0.08 in at 104 ^{o}F for both 281 S1 and 281 N1, as shown in Table 4. Thus, both mixes are stable. However, the field measurements show more rutting in 281 N1 than in 281 S1. A decision was made to perform the Hamburg tests at two temperatures (104 ^{o}F and 122 ^{o}F) and to continue to 99,900 passes, which is the maximum number the HWTD can apply. From seismic testing, observation during coring, and MDD data, it was found that the properties of AC layers are significantly different between the top and bottom of the AC. Thus, to quantify the rutting potential of top and bottom layers, the research team prepared two specimens for each core. The top and bottom layers denote specimens from the top 2.4 in. and the next 2.4 in. Although the HWTD was programmed to conduct the test up to 99,900 passes, the test was programmed to be terminated automatically when specimens reached 0.79 in. on either side of the wheel track. Experience shows that two specimens virtually never fail at the same number of passes with a 0.79 in. rut depth (Izzo and Tahmoressi 1999). Table 5 presents the test results from 281 N1 and 281 S1 at 104 ^{o}F and 122 ^{o}F. The numbers of passes when the specimens reached 0.8 in. deformation are listed in Table 5. It was observed that the top layer of 281 N1 and 281 S1 yielded no significant difference at either temperature. The bottom layers of 281 N1 and 281 S1 had a higher rutting rate than the top layers. The bottom layer of the northbound specimens yielded the highest rate of rutting at both temperatures.

Table 2 Rutting and Percent Rutting Contributed by Surface, Base, and Subgrade Layers in 281 S1 and 281 N1 (1 inch=25.4mm)

281 S1 MLS Axles	MLS Measured Average Overall Rutting (inches)	Rutting Contributed by AC (inches)	Rutting Contributed by AC (%)	Rutting Contributed by Base & Subgrade (inches)	Rutting Contributed by Base & Subgrade (%)
0	0	0	0	0	0
20,000	0.01	0.01	46.9	0.01	53.08
40,000	0.05	0.04	80.7	0.00	19.35
80,000	0.03	0.02	62.7	0.01	37.34
300,000	0.04	0.03	64.9	0.02	35.07
450,000	0.08	0.05	70.7	0.02	29.3
600,000	0.09	0.07	74.1	0.02	25.86
750,000	0.10	0.07	72.0	0.03	27.99
900,000	0.13	0.10	72.8	0.04	27.19
1,050,000	0.15	0.10	67.7	0.05	32.34
1,200,000	0.16	0.11	70.8	0.05	29.22
1,350,000	0.16	0.11	70.9	0.05	29.07
1,500,000	0.17	0.12	71.9	0.05	28.12
281 N1 MLS Axles	MLS Measured Average Overall Rutting (inches)	Rutting Contributed by AC (inches)	Rutting Contributed by AC (%)	Rutting Contributed by Base & Subgrade (inches)	Rutting Contributed by Base & Subgrade (%)
0	0	0	0	0	0
20,000	0.09	0.08	84.2	0.01	15.78
40,000	0.10	0.08	78.9	0.02	21.09
80,000	0.11	0.08	75.4	0.03	24.63
150,000	0.18	0.11	64.4	0.06	35.63
300,000	0.29	0.23	80.8	0.06	19.24
450,000	0.34	0.27	78.9	0.07	21.15
600,000	0.40	0.31	77.5	0.09	22.53

Table 3 Layer Rutting for Pads 281 N1 and 281 S1 at the End of 600,000 Axle Repetitions (1 inch=25.4mm)

	281 N1 (inches)	281 S1 (inches)
Top AC, 3.5 in	0.17	0.06
Bottom AC, 3.75 - 4.5 in	0.06	0.01
Base and Subgrade	0.10	0.02
Surface Rutting	0.33	0.09

Table 4 Comparison of the Rutting Potential Using the Hamburg Wheel-Tracking Device (Rutting up to 20,000 Passes) (1 inch=25.4mm)

		281S (inches)			281N (inches)		
		Left	Right	Average	Left	Right	Average
Top	104F	0.09	0.07	0.08	0.08	0.09	0.08
	122F	0.14	0.12	0.13	0.13	0.12	0.13
Bottom	104F	0.08	0.06	0.07	0.47	0.29	0.38
	122F	0.42	0.55	0.48	0.41	0.79	0.60

Table 5 Comparison of the Rutting Potential Using the Hamburg Wheel-Tracking Device [Number of Passes (xxx) up to 99,000 Passes] (1 inch=25.4mm)

		281S(inches)			281N(inches)		
		Left	Right	Average	Left	Right	Average
Top	104F	0.12 (99900)	0.10 (99900)	0.11 (99900)	0.11 (99000)	0.12 (99000)	0.12 (99000)
	122F	0.78 (54000)	0.53 (54000)	0.66 (54000)	0.79 (69100)	0.74 (69100)	0.76 (69100)
Bottom	104F	0.79 (97000)	0.71 (97000)	0.75 (97000)	0.78 (26000)	0.35 (26000)	0.57 (26000)
	122F	0.67 (30200)	0.78 (30200)	0.73 (30200)	0.41 (17800)	0.79 (17800)	0.60 (17800)

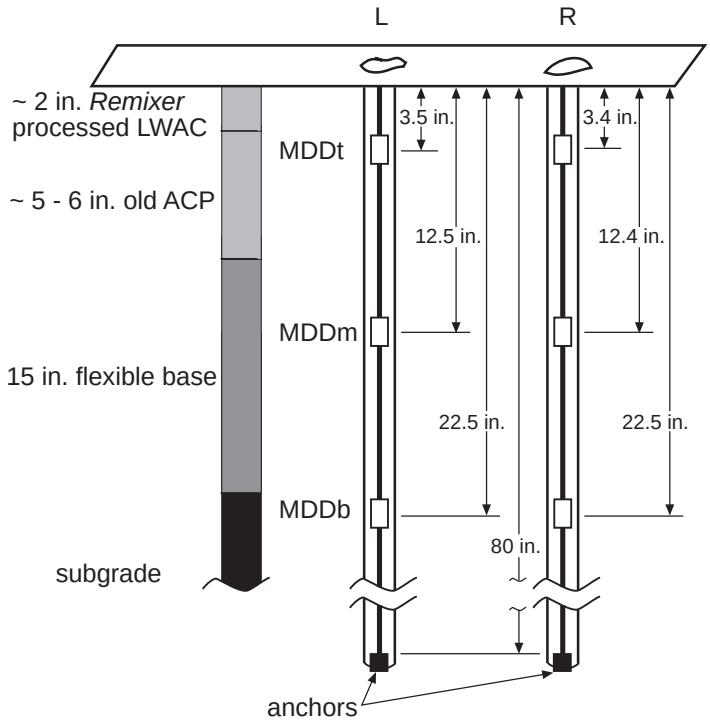

A

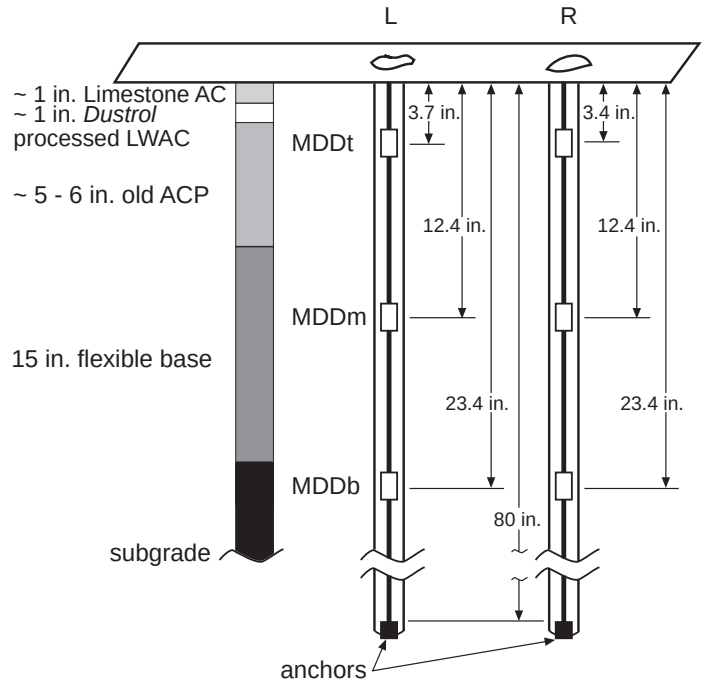

B

Figure 23 MDD and Pavement Layer Depths, (A) 281 S1 and (B) 281 N1

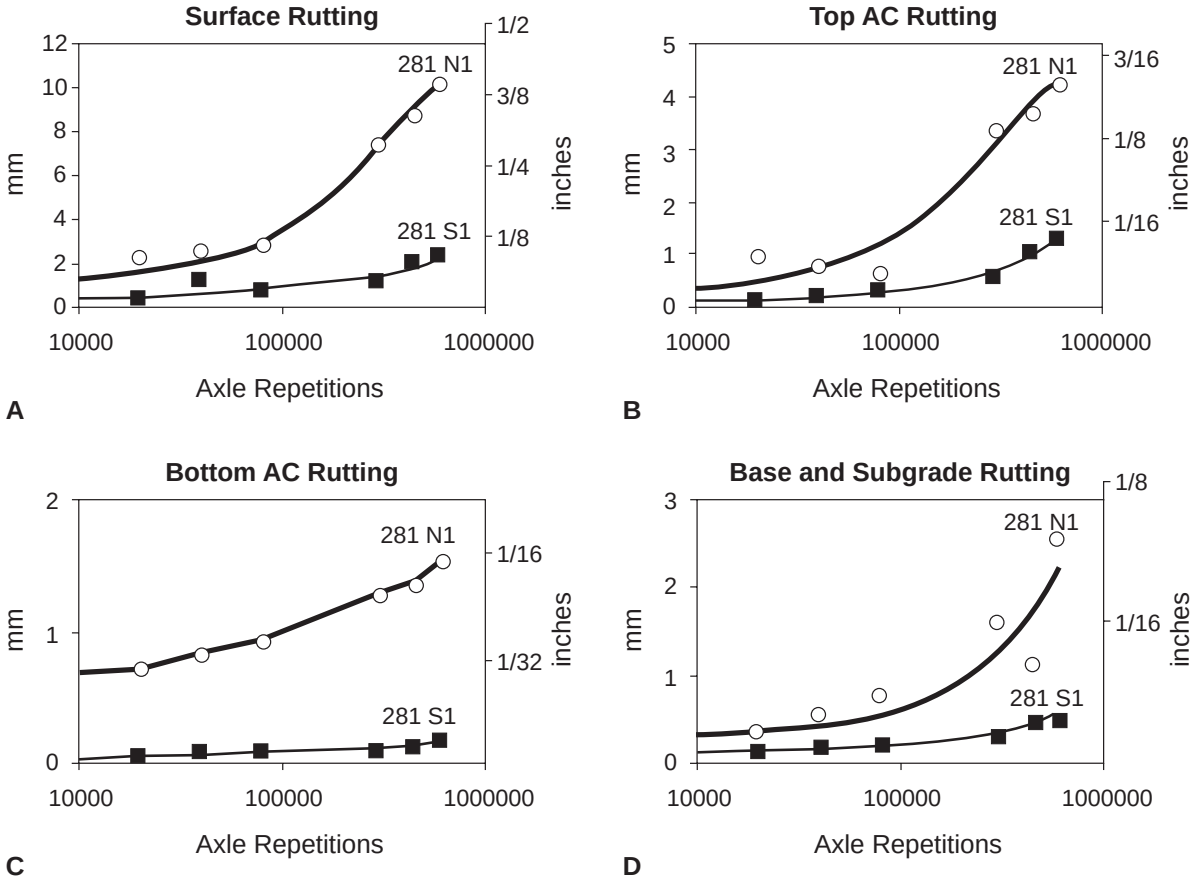

Figure 24 Comparison of Layer Rutting between 281 S1 and 281 N1, (A) Top AC, (B) Bottom AC, (C) Base and Subgrade, and (D) Surface

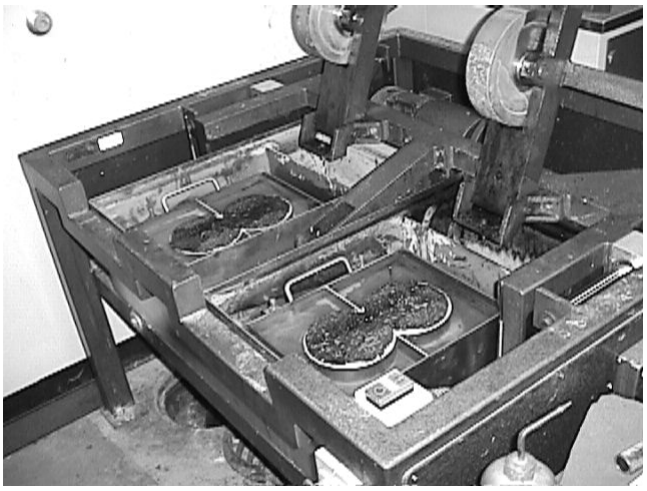

Figure 25 Hamburg Wheel-Tracking Device

PAVEMENT PERFORMANCE

Performance of the two pavements was established in terms of rutting, cracking, stripping, susceptibility to water damage, and behavior under high temperature trafficking.

Rutting

The primary distress evident on the Jacksboro test sections was rutting of the asphalt layer immediately under the surface layer. Total rutting was determined by measuring the deformation at the asphalt pavement surface. It can be defined by topographical coordinates or some arbitrary measure, such as the gap below a straightedge straddled across the rut. In the latter case, the straightedge could be placed with its extreme end points resting on the virgin pavement surface or resting on top of the highest points of the pavement surface.

Surface rut depth development at the MDD location (14.85 ft [4.5 m] line) is presented in Figures 26A and 26B for 281 S1 and 281 N1, respectively. Transverse profiles were measured from 0 ft to 9.9 ft (0 m to 3 m), or from the left edge of the test pad to the right edge. Both the MDD transient responses and the permanent deformations indicated that the majority of the deformation occurred in the top asphalt layer. Figures 27A and 27B show the rut development at specific locations along the test pad with trafficking. These ruts were determined by applying the above definition. With the exception of the trends manifested at the 14.85 ft (4.5 m) line, the rutting in the right wheel path was consistently greater than that in the left. A computation of the mean maximum ruts between the 9.9 ft to 29.7 ft (3 m and 9 m) grid lines was made. It was found that the rut in the right wheel path was about 45 percent greater than that in the left.

After 1 million repetitions on 281 S1, the rate of rutting for underlying pavement layers decreased because the temperature was lower during this testing period and because the pavement began to dry out after the rainfall period. The test passed 1 million repetitions in mid-September. FWD, MDD, and rutting data show that the rate of pavement deterioration decreases after 1 million axles. This finding is probably a result of strain hardening and because the temperature and pavement moisture levels were lower.

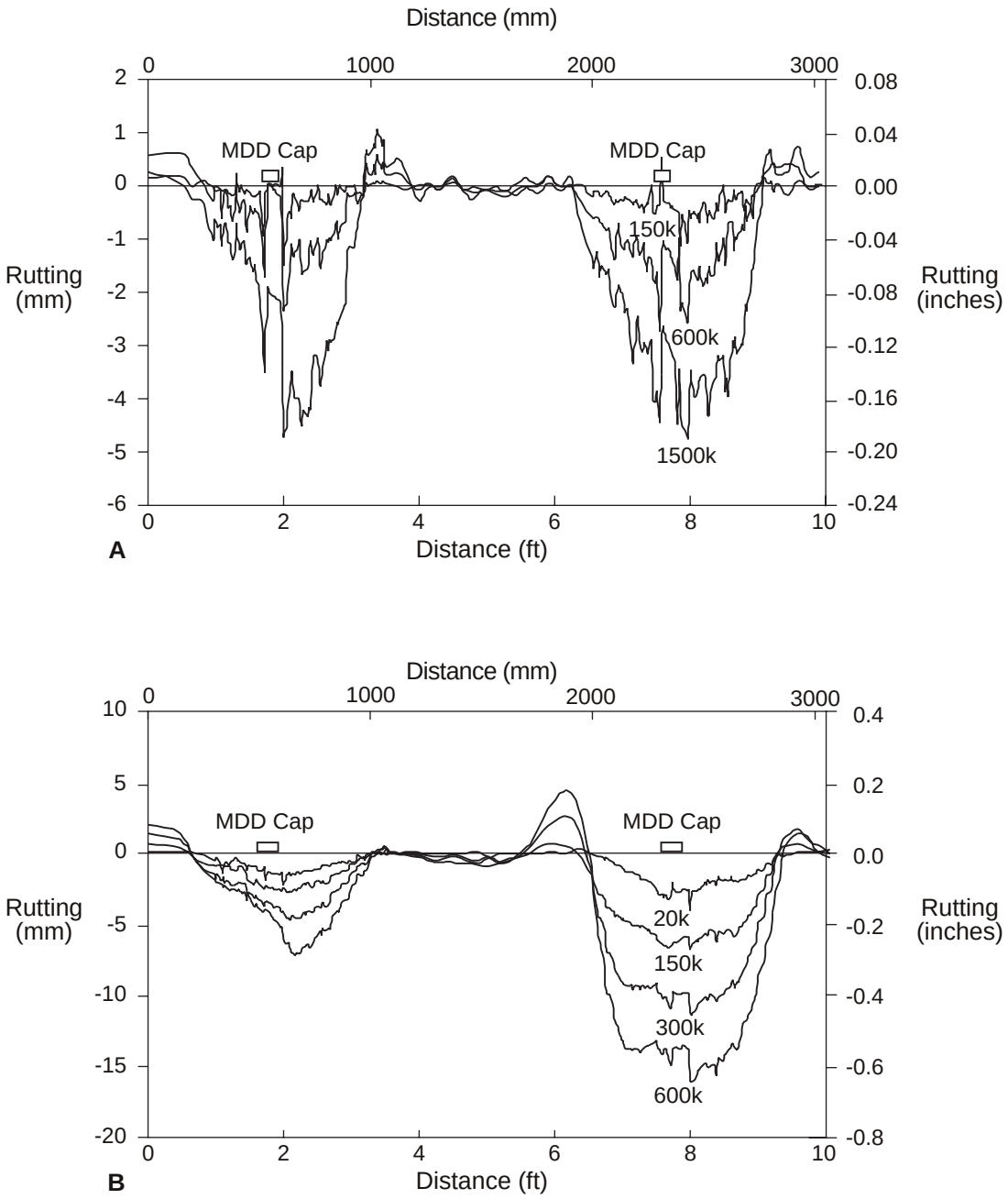

Figure 26 Surface Rut Development, (A) 281 S1 and (B) 281 N1 (1 mm = 0.04 in.)

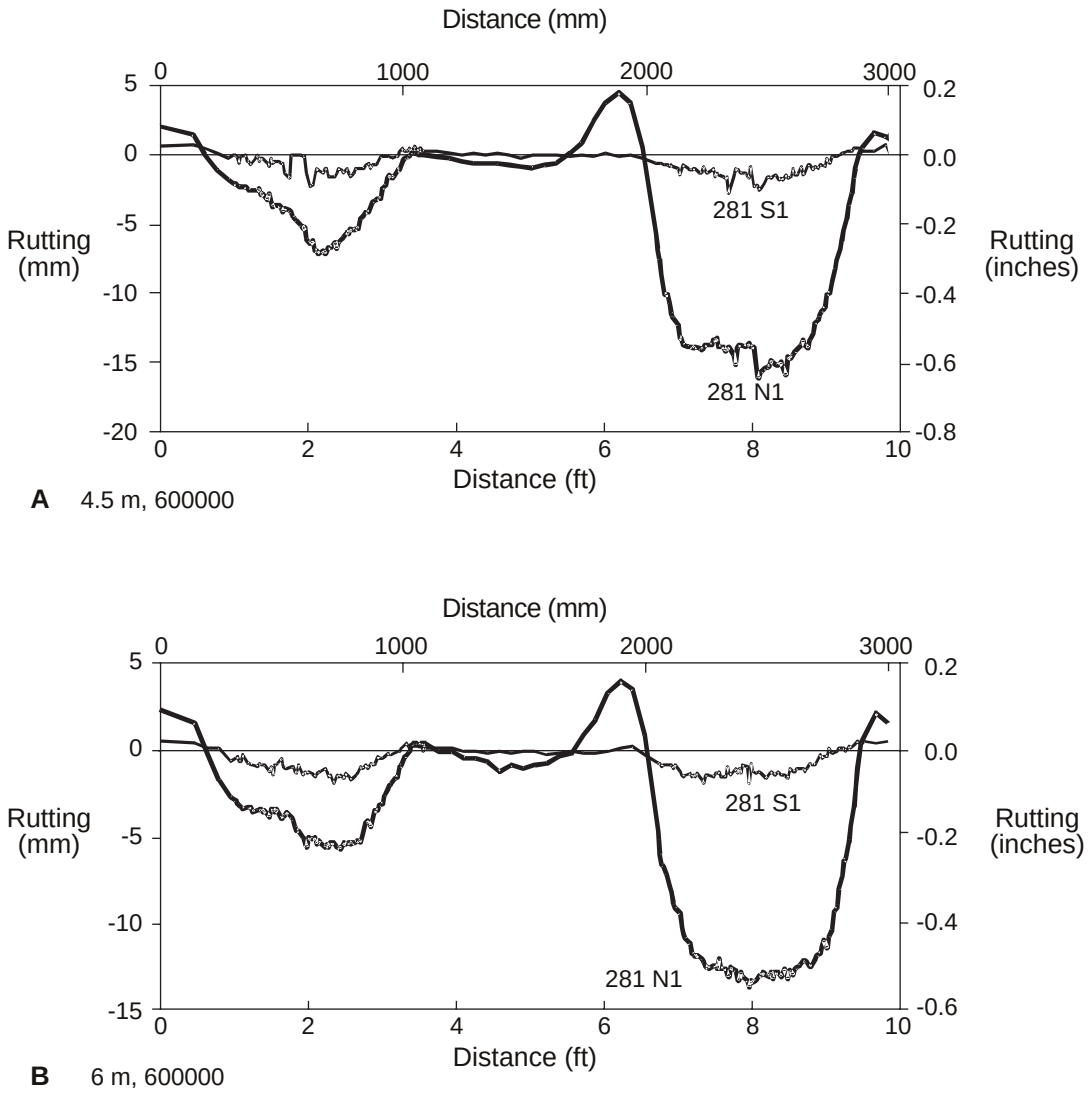

Figure 27 Comparison of Surface Rutting at the End of 600,000 Axle Repetitions, (A) 4.5 m and (B) 6 m (1 mm = 0.04 in., 1 m=3.28 ft)

Because the test pavement 281 S1 had carried the equivalent of 8 years of traffic in accelerated form without severe distress, it may be reasoned that the 1.5 million axle repetitions applied to the pavement is equivalent to 8 years of conventional traffic in the region.

Cracking

No visible load-related cracking was found in either test section. However, thermal surface transverse cracks were evident in both test pads prior to MLS trafficking. Distress in the form of micro-fracturing and subsequent longitudinal and alligator cracking of the overlay was observed in the outside lane. These observations are believed to be a result of stripping of the underlying LWAC.

VESYS PREDICTIONS OF RUTTING

The mechanistic rutting model VESYS (Kenis 1977) was used to predict the remaining life of 281 S1 and 281 N1, because the testing on 281 S1 and 281 N1 was terminated at different axle repetitions. In addition, the bottom AC of 281 N1 appeared to be weaker than that of 281 S1. The lack of support by this lower layer wou1d affect the performance of the top layer. The VESYS program was beneficial in this case as an analytical tool to determine the effectiveness of the Remixer and Dustrol processes.

The deformation of the respective layers, as determined from MDD (Table 2), and surface rut depths at different axle repetitions were used to calibrate the VESYS input parameters. The calibrated input parameters were then used to predict the remaining life of 281 S1 and 281 N1 beyond the terminated axle repetitions. Furthermore, to determine the effectiveness of the Remixer and Dustrol processes, the research team conducted comparative studies using the same set of input parameters for the underlying layers.

Input parameters for the VESYS program were first derived from repetitive triaxial tests and field FWD data. The rutting in each individual layer can be computed with adjustment to the VESYS analysis procedure. For simplicity, all comparisons were made for a two-layer system—that is, an AC layer and a subsystem (e.g., base and subgrade). Through several trial runs, a set of α, μ, and other material inputs was found to adequately describe the rutting behavior through the VESYS program. Laboratory repetitive triaxial tests were conducted on the AC cores to determine α and μ values. These α and μ values, together with material (e.g., thickness and stiffness), weather, and traffic parameters, were used in VESYS3AM to predict the rutting. Modifications of α and μ values were needed in order to match field measurements. Note that no repetitive triaxial tests were conducted for the base and subgrade materials to determine α and μ values. The α and μ values used in the study for base and subgrade were obtained from Kenis' recommendation (Kenis 1997) and several iterative trial runs. Detailed information about VESYS analyses can be also found in Chen et al. (1999).

Characterizing the rutting contributed by a specific pavement layer is an important task when a performance model such as VESYS is used. The α and μ values obtained from the repetitive triaxial tests at 104 ^{o}F for 281 S1 and 281 N1 are given in Table 6. Repetitive triaxial tests were conducted at two different temperatures, 68 ^{o}F and 104 ^{o}F. Interpolation and extrapolation were required to find α and μ at other temperatures. In the thermocouples installed in both test sites of US 281, the pavement temperatures prevailing during the test periods ranged from 60 ^{o}F to 95 ^{o}F. A decision was made to use 60 ^{o}F, 78 ^{o}F, 95 ^{o}F, and 86 ^{o}F to represent the mean four-season temperatures for both US 281 test sites. Table 7 shows the calibrated and adjusted α and μ values for 281 S1 and 281 N1. Table 8 illustrates the moduli used in the analyses.

Calculation of Layer Rutting

It is very important that the set of α and μ values not only meets the total surface rutting, but also that it matches individual layer rutting. The same set of parameters was used to predict the permanent deformations at different stages of trafficking in order to enhance confidence in the analysis. The predictions match well with field measurements at various test

stages, as shown in Figures 28 and 29 for 281 N1 and 281 S1, respectively. The input parameters used are presented in Tables 7 and 8. In the analyses, the AC was modeled as two layers to reflect the differences in material properties. It was observed that the AC layer was the primary contributor to the total surface rutting for both test pads. Table 2 presents the MLS-measured rutting and the percentage of rutting contributed by the AC, base, and subgrade layers for 281 S1 and 281 N1.

From 20,000 to 500,000 axles, the AC of 281 S1 contributes approximately 70 percent of overall surface rutting, while the AC in 281 N1 contributes approximately 75 percent, as measured by MDDs. It was concluded that the AC was the primary cause of the rutting of both the northbound and southbound lanes of US 281. Efforts were made to examine the source of rutting in the AC layer. It was found that approximately 9 percent of the total rutting in 281 S1 was from the lower AC, but for the same layer 19 percent of the rutting was found in 281 N1, as shown in Table 3. Nazarian et al. (1999) reported that the stiffness of the upper and lower AC of the northbound pads was 30 percent and 40 percent, respectively, lower than that of the southbound pads. Thus, both upper and lower AC layers in the northbound pads had higher rutting than the southbound pads. After 600,000 axle repetitions, average surface ruttings of 91 and 398 mils were recorded for 281 S1 and 281 N1, respectively. The top 3.5 in. of 281 S1 and 281 N1 yielded 64 and 236 mils of rutting, respectively.

PREDICTION OF REMAINING LIFE

The successful calibration of the VESYS rutting performance model with the field measurements provided an opportunity to attempt a remaining life prediction by using the same set of calibrated input parameters. With this set and any given number of axle repetitions the amount of rutting can be computed. Several runs with different axle repetitions were required to reach a surface rutting of 1 in. The results of the extrapolation for 281 S1 and 281 N1, using the parameters presented above, are shown in Figure 30. The remaining life for a specified criterion (either 0.5 in. or 0.75 in.) can be obtained from this figure for these two pavement sections. It is apparent that 281 N1 had more rutting than 281 S1 at any given phase of loading.

COMPARISON OF THE REMIXER AND DUSTROL REHAB PROCESSES

To compare the effectiveness of the two rehab processes, the researchers performed an analysis using the parameters of the underlying layers of 281 S1 instead of the parameters of the underlying layers of 281 N1. The only difference in the comparative analysis was the input parameters of the top layers. The comparisons are given in Figure 31A, 31B, 31C, and 31D for surface rutting, top AC rutting, bottom AC rutting, and base and subgrade rutting. It is evident from Figure 31 that even if 281 N1 had had the same underlying materials as 281 S1, the rutting performance in 281 N1 would have been poorer than that in 281 S1. Based on the VESYS analyses, it can be concluded that the Remixer process performed better than the Dustrol process in terms of rutting.

Table 6 AC α and μ Obtained by Repetitive Triaxial Tests at 104 ^{o}F

TEST SITES	281 N1		281 S1	
AC Layer	Upper	Lower	Upper	Lower
μ	0.12	0.14	0.09	0.15
α	0.53	0.57	0.53	0.64

Table 7 The Rutting Parameters α and μ for 281 N1 and 281 S1

281 N1					
		TEMPERATURE (^{o}F)			
LAYER	RUTTING PARAMETER	60	78	95	86
1 (Top AC, 3.5 in.)	μ	0.45	0.46	0.52	0.48
	α	0.70	0.69	0.67	0.68
2 (Bottom AC, 4.4 in.)	μ	0.20	0.19	0.25	0.21
	α	0.74	0.72	0.70	0.71
3 (Base, 15 in.)	μ	0.22	0.22	0.22	0.22
	α	0.75	0.75	0.75	0.75
4 (Subgrade, 53 in.)	μ	0.04	0.04	0.04	0.04
	α	0.75	0.75	0.75	0.75
5 (Bedrock)	μ	0.04	0.04	0.04	0.04
	α	0.75	0.75	0.75	0.75
281 S1					
		TEMPERATURE (^{o}F)			
LAYER	RUTTING PARAMETER	60	78	95	86
1 (Top AC, 3.5 in.)	μ	0.16	0.17	0.22	0.20
	α	0.69	0.68	0.66	0.67
2 (Bottom AC, 3.7 in.)	μ	0.05	0.06	0.07	0.06
	α	0.78	0.76	0.73	0.75
3 (Base, 15 in.)	μ	0.068	0.068	0.068	0.068
	α	0.75	0.75	0.75	0.75
4 (Subgrade, 81 in.)	μ	0.04	0.04	0.04	0.04
	α	0.75	0.75	0.75	0.75
5 (Bedrock)	μ	0.04	0.04	0.04	0.04
	α	0.75	0.75	0.75	0.75

Table 8 AC Moduli at Four Seasons for 281 N1 and 281 S1
AC Moduli x 1 000 psi

281N1	60 (F)	78 (F)	95 (F)	86 (F)
AC, 3.5 inch	718	378	234	298
AC, 4.5 inch	423	223	138	176
Base, 15 inch	38	38	38	38
Subgrade, 53 inch	8	8	8	8
Bedrock	500	500	500	500
281S1	60 (F)	78 (F)	95 (F)	86 (F)
AC, 3.5 inch	1325	698	431	549
AC, 3.75 inch	898	473	292	372
Base, 15 inch	38	38	38	38
Subgrade,81 inch	8	8	8	8
Bedrock	500	500	500	500

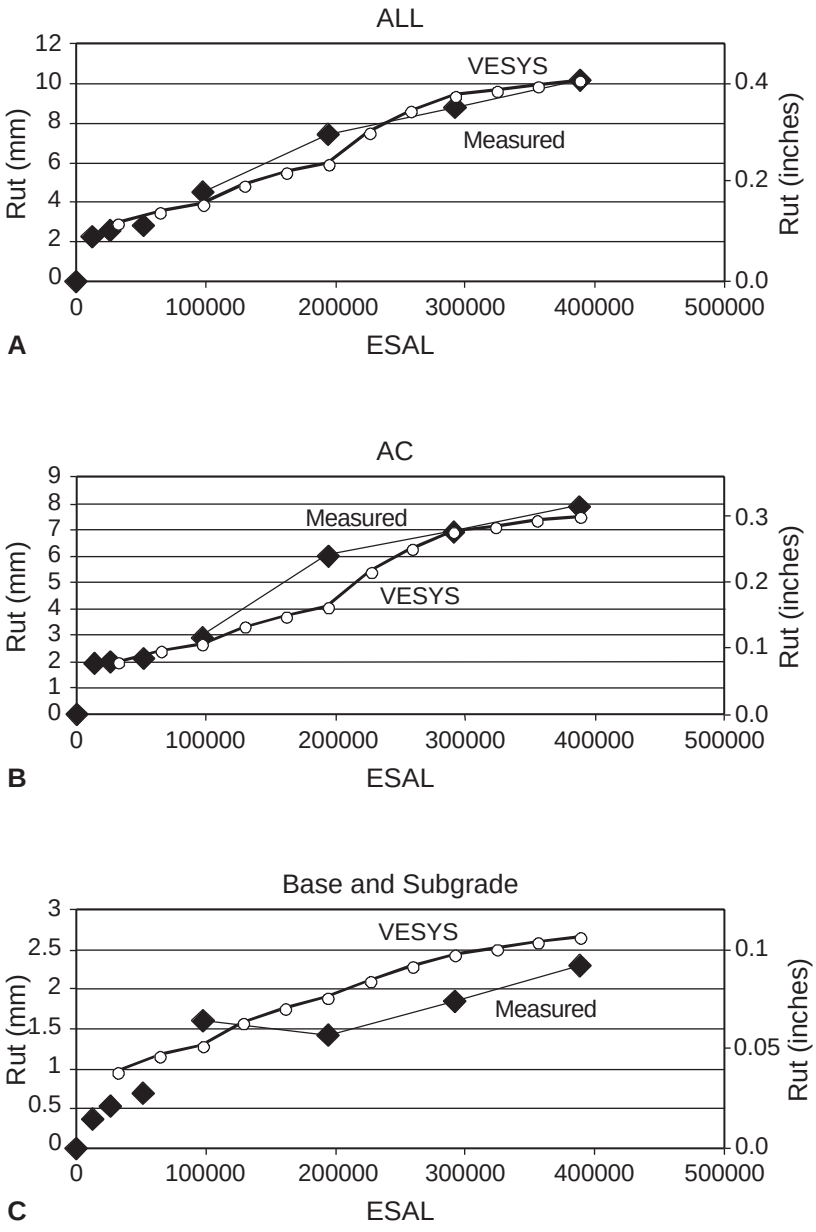

Note: 1 mm = 0.4 in.

Figure 28 Comparisons of VESYS Predictions and Measurements for 281 N1, (A) Surface Overall Rutting, (B) AC Rutting, and (C) Base and Subgrade Rutting

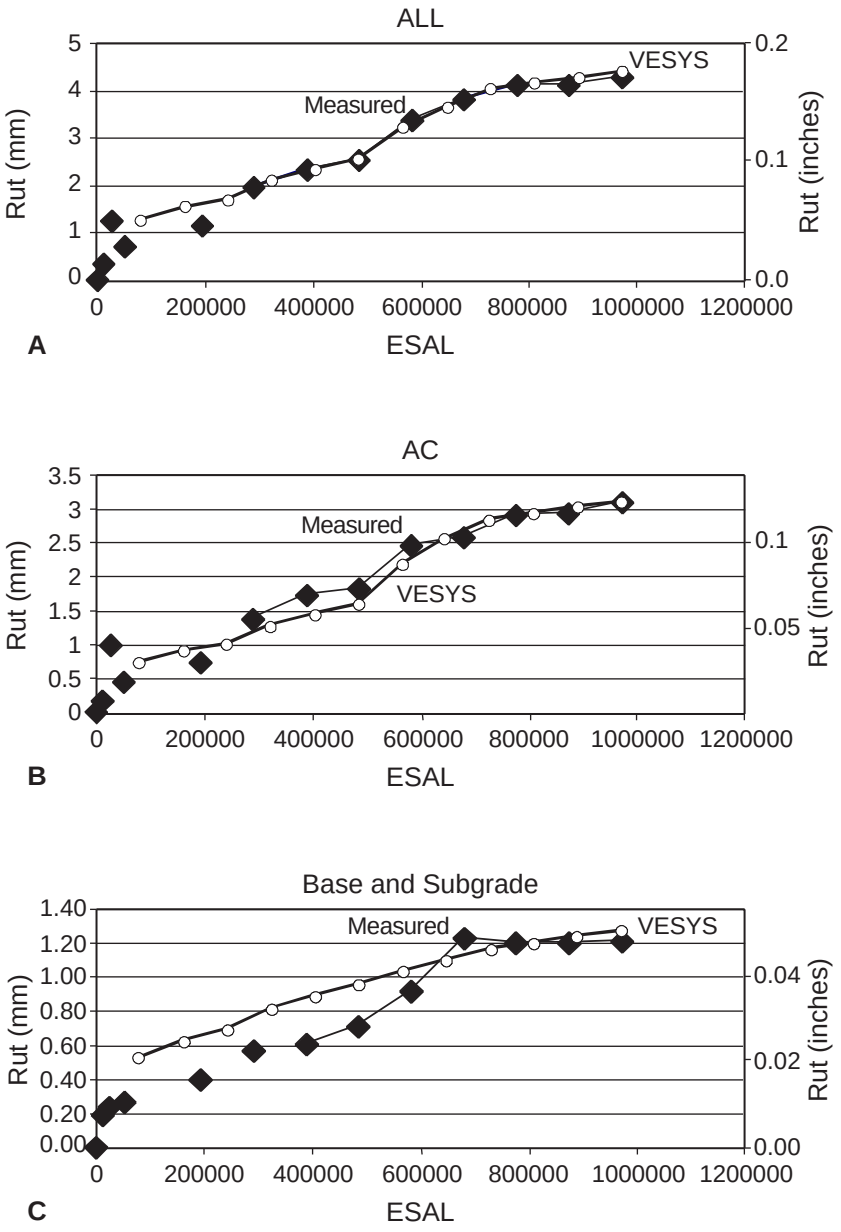

Figure 29 Comparisons of VESYS Predictions and Measurements for 281 S1, (A) Surface Overall Rutting, (B) AC Rutting, and (C) Base and Subgrade Rutting (1 mm = 0.4 in.)

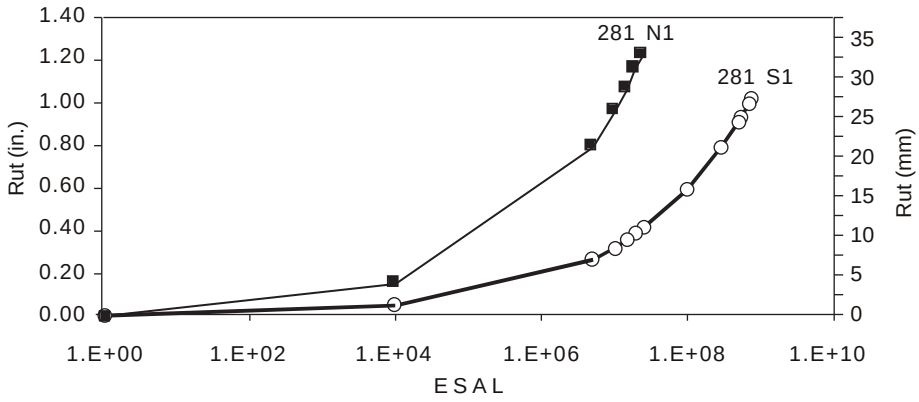

Figure 30 Remaining Life Predictions

SUSCEPTIBILITY TO STRIPPING AND PERFORMANCE UNDER HIGH TEMPERATURE TRAFFICKING

The stripping was discovered during diagnostic coring in the proximity of the MLS. It is probably linked to trapped water at the interface between the LWAC and the underlying limestone AC. The distress was exacerbated by cracks owing to the thermal stresses reflecting through the layers. It was apparent that for the rehabilitated layer to be effective, it needed to be supported by structurally sound underlying layers. This distress in the adjacent in-service outer lane pavement was already becoming manifest after less than 3 years of service life.

The test pavement, in service since mid-1957, had had three major overlay-type rehabilitations prior to the recent overlay. However, the record indicated no difference in overlay rehabilitation between the inside and outside lanes. The pavement structure of the outside lane appears to be weaker than that of the inside lane, a result of it having carried roughly 90 percent of the regular traffic since 1957.

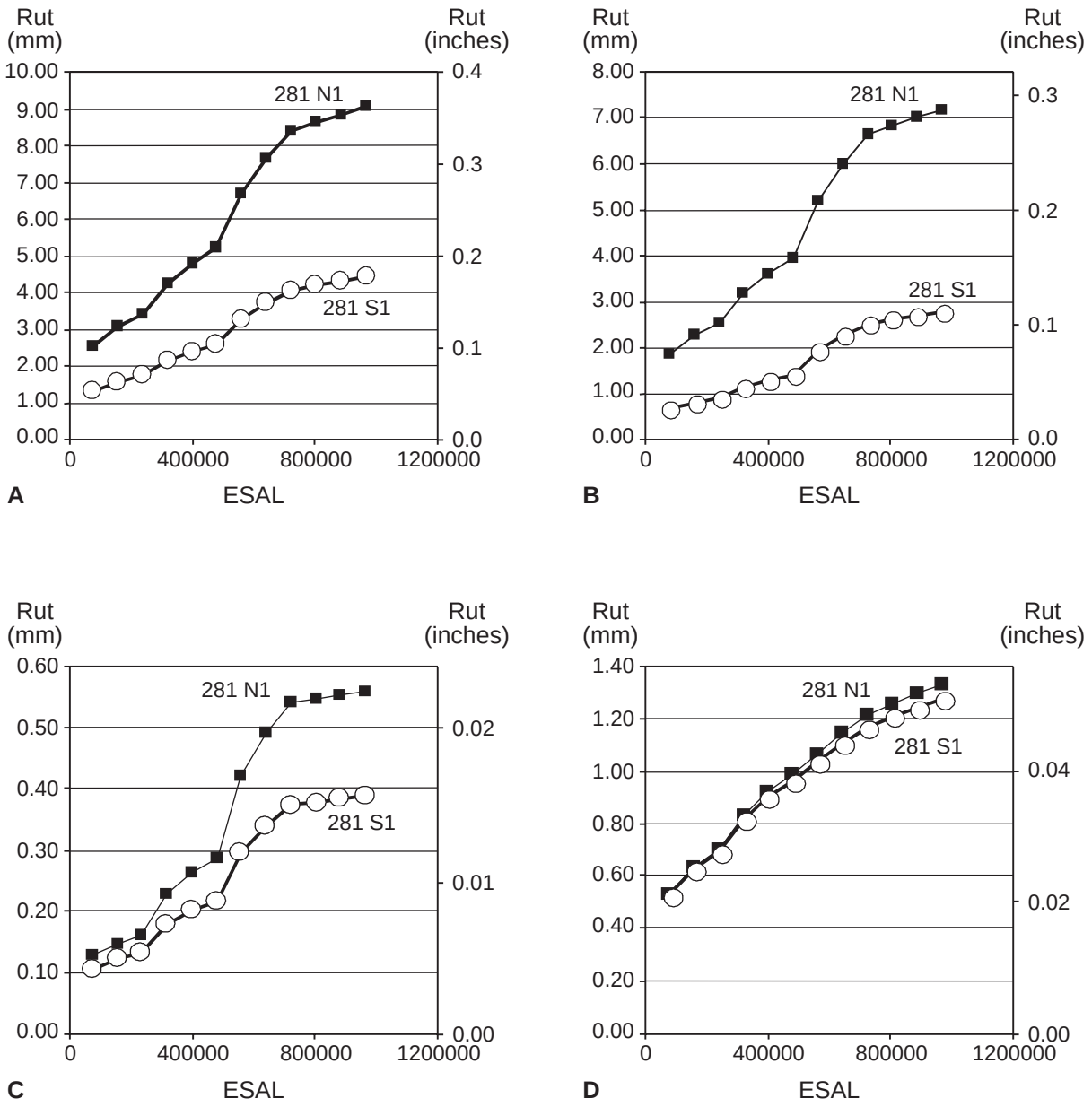

Figure 31 Comparison of VESYS Predictions between 281 S1 and 281 N1, (A) Surface Overall Rutting, (B) Top AC Rutting, (C) Bottom AC Rutting, and (D) Base and Subgrade Rutting (1 mm = 0.4 in.)

Separate projects were undertaken to investigate these phenomena and to evaluate the performance of the upper layers (4 in.) of the pavement under high temperature conditions and wet trafficking. The MMLS3 was used for the investigation. Trafficking was performed at

120 °F (50 °C) for the high temperature test and at 80 °F (30 °C) for the wet test. In the latter case the surface was inundated during the entire test. Performance was measured in terms of

- drop in PSPA moduli,
- rutting,
- indirect Tensile Strength (ITS)
- tensile Strength Ratio (TSR), and
- fatigue performance in ITS-mode.

These investigations are detailed in Reports 1814-2 and 1814-3. It is noteworthy that the Remixer process performed somewhat better under wet conditions, although both processes were susceptible to water damage. By contrast, the Dustrol process appeared to perform better than the Remixer process in terms of microfracturing. Both processes exhibited susceptibility to stripping under wet trafficking. Under high temperature trafficking, the Remixer process outperformed the Dustrol process.

SYNTHESIS OF FINDINGS PERTAINING TO PAVEMENT RUTTING PERFORMANCE

As presented above, initial FWD deflections (prior to MLS loading) were higher in the northbound than in the southbound test pads. This finding indicates that the southbound pavement structure is stronger than the northbound. The PSPA data also yielded higher velocity (moduli) values in the southbound for both top and bottom AC layers. However, laboratory Hamburg test results gave only a small variation between the performance of the upper 4.9 in. of southbound and northbound sections. In situ instrumentation (MDD) indicated that all layers in the northbound pad had greater rut depths. SPA, MDD, and Hamburg test results all indicated that the bottom AC layer of 281 N1 was weaker than that of 281 S1. It was therefore reasoned that the lack of support on the lower layer of 281 N1 affected the performance of the top layer of 281 N1 (Dustrol). From the mechanistic rutting model VESYS, using the same set of input parameters for underlying layers, the researchers found that the Remixer process performed better than the Dustrol process in terms of rutting.

Although the MLS tests on 281 S1 and 281 N1 were conducted during similar seasons, the average mid-depth temperature was approximately 7 ºF higher for the northbound pad. Thus, the higher rutting rate in the northbound section was owing not only to a weaker structure, but also to the higher temperature. When the effects of temperature and the underlying structural support were used to quantify the rutting performance of these rehab processes, it was found that, on average, the Remixer process rutted 0.14 in. after 1.5 million axle load applications. It was concluded that for the equivalent temperature, structural support, and load conditions, the Dustrol process would rut between 0.18 in. and 0.2 in.

Although the test was performed without any attempt to control environmental conditions, the MLS shell moderated temperature and moisture fluctuations to some degree. The temperature variation was rather limited. For test pad 281 S1, an average of 82.4 ºF with a coefficient of variation of 12.5 percent was measured and contrasted to the active highway, where the pavement was subject to the full impact of seasonal variation. In addition, the ingress of water into pad 281 S1 during rainfall was limited owing to the sheltering effect of the MLS.

In fact, the greater portion of the trafficking (90 percent) occurred without rainfall. It was therefore not surprising that the southbound pavement subject to conventional traffic had experienced far greater loss of stiffness and exhibited surface cracking when it was investigated closely. The average temperature during testing of pad 281 N1 was 89 ºF.

Distress in the form of wear and flushing of the binder was evident at the termination of the tests of 281 S1 and 281 N1. It is believed that this is because of the migration of the binder from the bottom layer of asphalt owing to trafficking, though this was not validated.

On the face value of the findings, and more particularly on the basis of the rut performance shown in Figure 24, Remixer performed better than Dustrol. However, it was apparent that the complex nature of the system necessitated a quantitative evaluation of the findings. This is discussed in the next section.

A QUANTITATIVE ANALYSIS OF THE RUTTING DAMAGE

The quantitative analysis of the rutting performance is based on the assumption that the rut depth is determined by the cumulative effects of the following factors:

- temperature (F_t)
- structural response (F_s)
- material compliance after processing (F_m)
- wheel load (F_l)

Furthermore, it is accepted that these effects occur concurrently.

The research team compared ruts in the different wheelpaths in terms of a *benchmark* pavement lane. In this research, the left-hand wheelpath of S1 (LWP S1) was selected as the benchmark lane, given that it had the least rutting. This choice does not influence the outcome.

Based on the principle of superposition, the total affected ruts of the respective pavement lanes, subjected to conditions differing from those of the benchmark pavement lane, may therefore be calculated as shown below:

The Total Affected Rut is defined as follows:

$$\text{Total Affected Rut(s)} = \alpha\left(F_t^{\beta_t} * F_s^{\beta_s} * F_m^{\beta_m} * F_l^{\beta_l} * F_{ltp}^{\beta}\right)BR \qquad (1)$$

Where BR = Benchmark Rut and α and β are modeling parameters.

Therefore log [Total Affected Rut(s)/BR]

$$= \log\alpha + \left(\beta_t \log F_t + \beta_s \log F_s + \beta_m \log F_m + \beta_l \log F_l + \beta_{tp} \log F_{tp}\right) \qquad (2)$$

The assumptions, with respect to each of the influence factors (temperature, structural response, material, and wheel load) and their quantification, are discussed below. For the sake of

expediency in demonstrating the principles, a somewhat simplified approach was followed in quantifying the influence factors.

Temperature

There are many ways of taking into account the influence of temperature. For the purpose of this analysis, the correction factor, for stiffness based on Sousa and Monismith as developed in the SASW studies, was used (Lee et al. 1997).

Structural Response

The FWD response prior to testing was used as the basis for determining input parameters for rehab remaining life curves as presented by Croney and Croney (1991). These curves express a relationship between performance life and deflection. The FWD deflections were 50 percent of the creep deflections used by Croney and Croney. This percentage was considered acceptable on the basis of extensive work by Lourens (1995) in South Africa. The performance life ratios were 2.2 and 2.5, based on initial FWD values of 9.8 mils, 12.6 mils, and 13.6 mils for pad 281 S1, pad 281 N1 (LWP), and pad 281 N1 (RWP), respectively. An analysis of the MDD data at 600 k and 1,500 k found that between 33 percent and 50 percent of the permanent deformation in the two test pads was in the old pavement structure, with most in the base.

Material Processing

Material processing was defined as a factor to take account of the effective difference in material response in terms of rutting as a result of the two processes. An extensive study of the material characteristics is reported elsewhere (Chen et al. 1998) and (Hugo et al. 1999). This was initially considered to be the most important influence on performance. As will be shown later, the structural response was the dominant factor.

Wheel Load

While the conventional power law was used, the exponent was not fixed at 4, based on serviceability (AASHO, 1962); it was instead determined from the measured rutting damage related to the load.

Analysis

As outlined previously, values of the respective influence factors were determined from the test findings, either by interpretation of the data or by calculation as discussed above. For the sake of simplicity, the α and β factors were initially set to equal 1.

Hence:

$$\text{Total Affected Rut(s)} = F_t * F_s * F_m * F_l * BR \qquad (3)$$

Where

BR = Benchmark Rut (0.063 in [1.6 mm] @ 600 k and 0.138 in [3.5 mm] @ 1500 k)
and log (Total Affected Rut (s)/BR) = $\left(\log F_t + \log F_s + \log F_m + \log F_l + \log F_{tp}\right)$ (4)

Table 9 shows the information and the results of the analysis

Table 9 Analysis and Interpretation of the Performance of Test Pads 281 S1 and 281 N1 (1 in. = 25.4 mm)

	281 S1						**281 N1**					
	LWP			RWP			LWP			RWP		
Benchmark Rut [BR] @ 600 k	**0.063 in**											
Ave Field Ruts @ 600 k	**0.063 in**			**0.098 in**			**0.307 in**			**0.531 in**		
Affected Rut/BR = *R*atio of measured rut relative to 281 S1 LWP			**1**			**1.56**			**4.87**			**8.44**
		F	1		F	1		F	1.22		F	1.22
		F_s	1		F_s	1		F_s	2.2		F_s	2.5
		F_m	1		F_m	1		F_m	{1.82}		F_m	{1.77}
		F_l	1		F_l	{1.56}		F_l	1		F_l	<1.56>
Benchmark Rut [BR @ 1500 k]	**0.138 in**											
Ave Field Ruts @ 1500 k	**0.138 in**			**0.189 in**			**(0.413 in)**			**(0.669in)**		
Affected Rut/BR = *R*atio of measured rut relative to 281 S1 LWP			**1**			**1.37**			**2.99**			**4.85**
		F	1		F	1		F	1.22		F	1.22
		F_s	1		F_s	1		F_s	2.2		F_s	2.5
		F_m	1		F_m	1		F_m	{1.12}		F_m	{1.16}
		F_l	1		F_l	{1.37}		F_l	1		F_l	<1.37>
Influence Factors (Normalized Relative to LWP 281 S1)												
Temperature correction of E [T] (*Aouad, 1993*)			1			1			1.22			1.22
Structure [S] Based on FWD (*Croney & Croney, 1991*)			1			1			2.2			2.5
Material Processing [M]			1			1			Calc. Calc.			Calc. Calc.
Load [L] Power Function			1			Calc. Calc.	——— ———		1 1	——— ———		Trans. Trans.
Load [L] $(1.07)^n$	After 600 k load applications F_l = 1.56, and n = 6.6 After 1500 k load applications F_l = 1.37, and n = 4.7											

{ }, Calc. = Calculated. ( ) = Extrapolated. < >, Trans. = Transferred. [BR] = Benchmark Rut

In the case of RWP S1, the load factor of the RWP was the only unknown in the equation. It could therefore be calculated. In a similar way the material influence in LWP-281 N1 was calculated. The calculation is shown as an example.

Calculation for determining F_m:

$\log(1.22) + \log(2.2) + \log(F_m) + \log(1) = \log(4.88)$ which results in $F_m = 1.82$

The proportional influence of the respective factors, to the increase in rutting by each factor, is then calculated as:

$\% F_t = \log(1.22) / \log(4.88) = 12.5\%$
$\% F_s = \log(2.2) / \log(4.88) = 49.7\%$
$\% F_m = \log(1.82) / \log(4.88) = 37.8\%$
$\% F_l = \log(1) / \log(4.88) = 0\%$

The other proportions in the table can be calculated in the same way.

After this it was possible to transfer the load factor of S1 to the RWP of N1. The material factor in the RWP could then be calculated. The results of the analysis for 281 N1 are shown in Table 10.

Table 10 Relative Contribution of Influence Factors towards Increase/Decrease in Rutting on US281 N1

	LWP		**RWP**	
N1 @ 600k	**Aff Rut-BR = 0.24 in**	**%**	**Aff Rut-BR = 0.47 in**	**%**
	Log F	100.06	Log F	99.90
F_t	0.09	12.54	0.09	9.32
F_s	0.34	49.74	0.40	42.96
F_m	0.26	37.78	0.25	26.77
F_l	0.00	0.00	0.19	20.85
Log Aff Rut/BR	0.69		0.93	
N1 @ 1500k	**Aff Rut-BR = 0.28 in**	**%**	**Aff Rut-BR = 0.53in**	**%**
	Log F	100.17	Log F	99.83
F_t	0.09	18.10	0.09	12.58
F_s	0.34	71.77	0.40	57.95
F_m	0.05	10.3	0.06	9.4
F_l	0.00	0.00	0.14	19.9
Log Aff Rut/BR	0.48		0.69	

Summary of the Performance Analysis

A summary of the preceding discussion of the tests is presented in Table 11. Two things are noteworthy in the analysis:

1. The average value of parameter *n* in the load damage power function, determined at 600 k and 1,500 k, was 5.7. This finding relates to the rutting distress found in the tests and not to serviceability loss.
2. The influence factors for Dustrol and Remixer can be compared. At the 600 k stage of pad 281 S1, F_m came to 1.82 and 1.77 for the left and right wheel paths, respectively. At 1,500 k, F_m came to 1.23 and 1.16 for the left and right wheel paths, respectively. From Table 10 it can be seen that 38 percent and 27 percent of the increase in rutting in the left and right wheel paths of 281 N1 were owing to material effects at 600 k. By contrast, 10 percent and 9 percent of increase in rutting in the LWP and RWP of 281 N1, was due to material effects at 1,500 k. An opposite trend is also apparent for the structural factor that increases with trafficking. The decrease in material effects may be because of stress hardening of the pavement with trafficking. Furthermore, the effects of the influence factors are not entirely independent of one another. Some part of the structure's influence may be taken up in the material influence and vice versa. The performance of the respective materials has to be weighed against the fact that the Remixer process was 22.5 percent more expensive than the Dustrol process.

Table 11 Factors Considered in Comparative Studies of 281 S1 and 281 N1 Performance

FACTOR	S1	N1	COMMENTS
• Climatic condition - Air temperature - Rainfall	 >	 > 	 Weather station
• Water sensitivity	*	*	Also see Hugo et al. (1999)
• Temperature susceptibility of performance		>	Validation to be done with MMLS Mk3
• FWD deflection prior to testing		>	The response indicated that 281 N1 was likely to have more distress than 281 S1.
• FWD deflection reduction during trafficking		>	Developed as expected. There was very little difference between the results of the two process.
• MDD permanent deformation - Left wheel path - Right wheel path	 >	 >>	Most deformation occurred in the surface layers and in the right wheel path.
• Rutting		>>	Still within specification, <3/4 in.
• Cracking	None √	None √	Microfracturing manifested in MMLS Mk3 testing for 281 N1 – see Hugo et al. (1999) Cracking manifested in south outer lane under regular conventional traffic
• SASW Modulus profile prior to testing		<	Probably owing to rehab process
• SASW Modulus reduction during trafficking	√	√	The SASW (and related SPA and PSPA) all indicated a reduction in modulus.
• PSI	√	√	Slope variance analysis using *Vertac* ~Quasi PSI
• Construction intensity		>	Equipment on site during construction
• Cost	>		22.5% more as per bids for experimental sections only

√ = Equal or similar, > = Greater or more, < = Less or little, * = Was investigated with the aid of MMLS Mk3 trafficking

CONCLUSIONS

This investigation is an excellent example of the complex nature of accelerated testing of in situ pavements. Normally, such pavements are composites constructed over extended periods of time. The Jacksboro pavement fell into this category. However, the sound substructure made it possible to gain valuable insight into the performance of two relatively thin rehab processes.

On the basis of the various data and assumptions presented, the following important conclusions were drawn:

1. The TDR results indicated that the test section possessed a satisfactory drainage system as defined by AASHTO. It took 4.5 hours to drain 50 percent of the water, which had infiltrated the section as a result of 0.75 in. rainfall.
2. The traffic wander pattern applied by the MLS is slightly more concentrated than what occurs under conventional traffic. The width of the MLS wander is approximately 35 in. The MLS applies 67 percent of traffic over most (22 in.) of the wheel path, with a peak of 83 percent near the center. Thus, owing to a higher concentration, the MLS may induce more damage per axle.
3. FWD and SASW tests both indicated that 281 S1 was stronger than the 281 N1. As expected, 281 S1 yielded less rutting than 281 N1.
4. MDD, SPA, and Hamburg test results indicated that the bottom AC layer of 281 N1 was weaker than 281 S1.
5. With both test pads, the bulk of rutting (about 63 percent at pad 281 S1's MDD location) occurred in the most recently constructed rehab and the immediately underlying lightweight ACP. On average, the aged underlying asphalt (>22 years) and base (>40 years) contributed about 30 percent to overall rutting, while the subgrade layers contributed about 7 percent to overall rutting. Most of the rutting occurred between 300 k and 1 million axles and during the summer months when temperatures and pavement moisture levels were substantially higher. During the following dryer and cooler weather period, the rutting trends were reduced. For pad 281 N1, about 35 percent of the rutting took place before 100 k axles.
6. The rutting performance was affected by temperature, the pavement structures, and rehab materials. In addition, a faulty load cell in the right WIM device caused the RWP to have a 7 percent higher load than the LWP. Through a progressive process of analysis, it was possible to quantify the effects of each of these factors. This analysis made it possible to determine the difference in rutting performance between the two processes quantitatively.
7. The quantitative analysis of rutting performance provided a reasonable evaluation of the difference in performance between two rehab processes. This analysis makes it possible to evaluate the cost differential between the two processes on a rational basis. Discounting for the influence of temperature, the difference in structural response, and the effect of the increased load in the right wheel path, only 38 percent and 27 percent of the rutting in the LWP and RWP of the Dustrol section (281 N1) were owing to material effects after 600 k axles. The increased rutting after 1,500 k axles, because of material effects only, was calculated to be 10 percent and 9 percent of the predicted final rut for the LWP and RWP in pad 281 N1. This finding has to be weighed against the fact that the Remixer process was about 22.5 percent more expensive.

8. The mechanistic rutting model VESYS was used to determine the effectiveness of the Remixer and Dustrol rehab processes, using the same set of input parameters for the underlying layers. It was found that the Remixer process performed better than the Dustrol process in terms of rutting.
9. Test pad 281 S1 carried the equivalent of 8 years of conventional traffic, in accelerated form, without severe rutting distress. This result was probably owing to the sound underlying structure, effective drainage system, and minimal ingress of surface water.
10. Despite the conditions and circumstances surrounding the MLS tests, it can be concluded that the Remixer rehabilitation process offers a rut-resistant layer, provided it is supported by a sound underlying structure. In view of this, the District Pavement Engineer was satisfied with the performance of this rehabilitation process.

In contrast to the satisfactory performance of the Remixer overlay, severe distress, in the form of longitudinal and alligator cracking, manifested itself in the outside lane adjacent to the test section during the execution of the 281 S1 test. The causes of this phenomenon were thought to be stripping of the underlying lightweight asphalt concrete (LWAC) and possible weakness of its underlying structure. The water susceptibility and effect of high temperature trafficking were subsequently investigated with the use of the third-scale Model Mobile Load Simulator (MMLS3). Overall, the Remixer process performed somewhat better than the Dustrol process. The tests and results are presented in Reports 1814-2 and 1814-3.

The purpose of this report has been to give a detailed presentation of the MLS investigation in Jacksboro, Texas, that compared two rehab strategies, Remixer and Dustrol. This information should be of use to other districts, to TxDOT, to AASHTO, and to other APT users. The TxMLS program has yielded a variety of products and has increased pavement engineering knowledge. Further value has been added through direct implementation of findings where appropriate. Based on the satisfactory performance of the Remixer rehab on its sound underlying structure, it was used on a section of US 175 in the Dallas District. However it was found later that the Remixer could not stop reflected cracking on the US 175 project.

REFERENCES

1. AASHO (1962), "The AASHO Road Test, Summary Report," Special Report 61 G; Highway Research Board, Washington, D.C.
2. Aschenbrener, T., Terrel, R. L., and Zamora, R. A. (1994) *Comparison of the Hamburg Wheel Tracking Device and the Environmental Conditioning System to Pavements of Known Stripping Performance*, Report No. CDOT-DTD-R-94-1, Colorado Department of Transportation, Denver, Colorado, January 1994.
3. Chen, Dar-Hao, Fults, K., and Murphy, M. (1997) "The Primary Results for the First TxMLS Test Pad," Transportation Research Board, *Transportation Research Record No. 1570*. pp. 30–38.
4. Chen, D-H., and Hugo, F. (1998) "Test Results and Analyses of the Full-Scale Accelerated Pavement Testing of TxMLS," *Journal of Transportation*, ASCE, Sept/Oct.
5. Chen, Dar-Hao, Lin, H., and Hugo, F. (2000) "Application of VESYS3AM in Characterization of Permanent Deformation," *International Journal of Pavement Engineering*, Vol. 1(3), pp. 171–192.
6. Hugo, F., Fults, K., Chen, D-H., De Fortier Smit, A., and Bilyeu, J. (1999) "An Overview of the TxMLS Program and Lessons Learned," CD-ROM, Proceedings of the International Conference on Accelerated Pavement Testing, Reno, Nevada, October 18–20.
7. Izzo, R. P., and Tahmoressi, M. (1999) "Evaluation of the Use of the Hamburg Wheel-Tracking Device for Moisture Susceptibility of Hot Mix Asphalt," Paper No. 99, accepted for presentation at the 78th Transportation Research Board Annual Meeting and Considered for the *Transportation Research Record*.
8. Kenis, W. J. (1977) "Predictive Design Procedures — A Design Method for Flexible Pavements Using the VESYS3AM Structural Subsystem," Proceedings, of the Fourth International Conference on the Structural Design of Asphalt Pavements, The University of Michigan, Ann Arbor, Vol. 1, pp. 101–147.
9. Kenis, W. J., and Wang, W. (1997) "Calibrating Mechanistic Flexible Pavement Rutting Models From Full Scale Accelerated Tests," Proceedings of the Eighth International Conference on Asphalt Pavements, Seattle, Washington, August, Vol. I, pp. 663–672.
10. Lee, C. E., and Pangburn, J. W. (1996) "Preliminary Research Findings on Traffic-Load Forecasting Using Weigh-in-Motion Data," Research Report 987-5, Center for Transportation Research, The University of Texas at Austin.
11. Lee, C. E., Shanker, P. R., and Izadmehr, B. (1983) "Lateral Placement of Trucks in Highway Lanes," Research Report 310-1F, Center for Transportation Research, The University of Texas at Austin.
12. Metcalf, J. B. (1996) "Application of Full-Scale Accelerated Pavement Testing," Synthesis of Highway Practice 235. National Cooperative Highway Research Program.

13. Nazarian, S., Yuan, D., Chen, Dar-Hao, and McDaniel, M. (1999) “Use of Seismic Methods in Monitoring Pavement Deterioration During Accelerated Pavement Testing with TxMLS,” CD-ROM, Proceedings of the International Conference on Accelerated Pavement Testing, Reno, Nevada, October 18–20.
14. Wimsatt, A., Scullion, T., Ragsdale, and Servos, S. (1998) “Use of Ground Penetrating Radar in Pavement Rehabilitation Strategy Selection and Pavement Condition Assessment” Paper 980729, presented at the 77th Annual Transportation Research Board Annual Meeting, published by SPIE (v. 3400) Third Conference on Nondestructive Testing.
15. Yuan, D., Nazarian, S., Chen, Dar-Hao, and Hugo, F. (1998) “Use of Seismic Pavement Analyzer to Monitor Degradation of Flexible Pavements Under Texas Mobile Load Simulator,” Transportation Research Board, *Transportation Research Record No. 1615*. pp. 3–10.